Fertilization Biology of Maize and Teosinte

by

CHI-CHIH WU

B.A., National Cheng-Kung University, Taiwan,1993

M.S., National Taiwan University, Taiwan, 1995

A thesis submitted to the

Faculty of the Graduate School of the

University of Colorado in partial fulfillment

of the requirements for the degree of

Doctor of Philosophy

Department of Ecology and Evolutionary Biology

2012

This thesis entitled:
Fertilization Biology of Maize and Teosinte
written by CHI-CHIH WU
has been approved for the Department of Ecology and Evolutionary Biology

Pamela K. Diggle

William E. Friedman

David W. Stock

William W. Adams III

Date _____

The final copy of this thesis has been examined by the signatories, and we find that both the content and the form meet acceptable presentation standards of scholarly work in the above mentioned discipline.

WU, CHI-CHIH (Ph.D., Ecology and Evolutionary Biology)

Fertilization Biology of Maize and Teosinte

Thesis directed by Prof. Pamela K. Diggle and Prof. William E. Friedman

By studying cultivated maize and its wild closest relative, Balsas teosinte, I addressed two questions: 1) female gametophyte development and double fertilization in Balsas teosinte (*Zea mays* subsp. *parviglumis*), and 2) kin recognition within a seed: the effect of genetic relatedness of an endosperm to its compatriot embryo on maize seed development.

First, over the course of maize evolution, domestication played a major role in the structural transition of the vegetative and reproductive characteristics that distinguish it from its closest wild relative, Balsas teosinte. Little is known, however, about impacts of the domestication process on the cellular features of the female gametophyte and the subsequent reproductive events after fertilization. The results show that the fertilization process of Balsas teosinte is basically similar to domesticated maize. In contrast with maize, many events associated with the development of the embryo and endosperm appear to be initiated earlier in Balsas teosinte. I propose that the relatively longer duration of the free nuclear endosperm phase in maize is correlated with the development of a larger fruit (kernel) and with a bigger endosperm compared with Balsas teosinte.

Second, as one of two sexually formed products resulting from double fertilization in angiosperms, the endosperm nourishes its compatriot embryo during seed development and/or germination and ultimately dies. Previous theoretical studies suggest that the coefficient of relatedness of an endosperm to an embryo in the same seed might determine the amount of resources ultimately available for the embryo during seed development. My results show that the degree of genetic relatedness of an endosperm to its compatriot embryo has a significant effect on embryo weight, but not on endosperm weight. Thus, the endosperm of heterofertilized seeds appears to behave less cooperatively with respect to resource transfer toward its

less-closely-related embryo compared to those in homofertilized seeds. This study provides key insights into the developmental and cooperative interactions between the endosperm and embryo as affected by coefficients of relatedness.

Dedication

This thesis is dedicated to my parent, teachers, and especially to my wife. Their enthusiasm continues to inspire me and their constant support has not allowed for anything other than success.

Acknowledgements

I would first like to gratefully and sincerely thank my advisors, Pamela Diggle and William (Ned) Friedman for their patience, guidance and insightful intellectual contributions to my researches and scientific writing. Their dedication to my process was invaluable to the completion of my degree. Additionally, their integrity and commitment to the pursuit of knowledge and understanding is truly inspirational.

I thank my committee members, David Stock, William Adams and Anne Sylvester, who have provided instruction and years of feedback. Without their guidance, I would not have completed this work.

Beyond my academic committee, I am also thankful for the support and help of all people in Pam's and Ned's lab: Jennifer Winther, Kirsten Ryerson, Amanda Redford, Jonathan Krieger, Noah Greenberg, Sam Holloway, Eric Madrid, Erin Bissell, Claire Lay, Robert Baker, April Randle, Becky Povilus, and Julien Bachelier. I appreciate their input into my thinking and writing as well as leisure outside lab works.

I thank the staff at the Department of Ecology and Evolutionary Biology of University of Colorado at Boulder for generous assistance and essential support: Bill Franz, Linda Bowden, Melissa Keller and Jill Skarstad. I thank Dr. John Basey. Without his patience for instruction on teaching, I can not accomplish the requirement of Graduate Teaching Assistant. I thank Thomas Lemieux for the guidance of growing corns in the greenhouse, University of Colorado.

I thank many researchers in maize researching community for their kindly consulting on maize breeding: Dr. Akio Kato (Kyoto Prefectural University), Dr. Stephen Stack (Colorado

State University), Dr. Patricia Bedinger (Colorado State University), Marty Sachs (Maize Genetics COOP Stock Center), Dr. William Tracy (University of Wisconsin-Madison), Dr. Susan Gabay-Laughnan (University of Illinois), and Dr. William Sheridan (University of North Dakota). I also thank Dr. Anne W. Sylvester, Dorothy Tuthill, Elinor Flores, and Dr. Anding Luo from University of Wyoming for their constant and generous support over the past few years in the maize research field.

Finally, I also sincerely thank all friends of Taiwanese (Formosa) Student Association, University of Colorado at Boulder. Their supports help me to recover from stresses of academic works.

This research was funded by the Ecology and Evolutionary Biology (EEB) Department Grant of the University of Colorado at Boulder, the Diggle's and Ned's labs.

Contents

Chapter

Tables

Table

Figures

Figure

Chapter 1

Female gametophyte development and double fertilization in Balsas teosinte, *Zea mays* subsp. *parviglumis* (Poaceae)

1.1 Abstract

Over the course of maize evolution, domestication played a major role in the structural transition of the vegetative and reproductive characteristics that distinguish it from its closest wild relative, *Zea mays* subsp. *parviglumis* (Balsas teosinte). Little is known, however, about impacts of the domestication process on the cellular features of the female gametophyte and the subsequent reproductive events after fertilization, even though they are essential components of plant sexual reproduction. In this study, we investigated the developmental and cellular features of the Balsas teosinte female gametophyte and early developing seed in order to unravel the key structural and evolutionary transitions of the reproductive process associated with the domestication of the ancestor of maize. Our results show that the female gametophyte of Balsas teosinte is a variation of the Polygonum type with proliferative antipodal cells and is similar to that of maize. The fertilization process of Balsas teosinte also is basically similar to domesticated maize. In contrast with maize, many events associated with the development of the embryo and endosperm appear to be initiated earlier in Balsas teosinte. Our study suggests that the pattern of female gametophyte development with antipodal proliferation is common among species and subspecies of *Zea* and evolved before maize domestication. In addition, we propose that the relatively longer duration of the free nuclear endosperm phase in maize is correlated with the development of a larger fruit (kernel

or caryopsis) and with a bigger endosperm compared with Balsas teosinte.

1.2 Introduction

Maize, *Zea mays* subsp. *mays*, is one of the most economically important crops for food and forage. The genus *Zea* comprises five species (*Z. diploperennis*, *Z. luxurians*, *Z. nicaraguensis*, *Z. perennis*, *Z. mays*) and four subspecies (*Z. mays* subsp. *huehuetenangensis*, *Z. mays* subsp. mexicana, *Z. mays* subsp. *parviglumis*, *Z. mays* subsp. *mays*) (Doebley and Iltis, 1980; Iltis and Doebley, 1980; Iltis and Benz, 2000; Doebley, 2003), and phylogenetic analyses of the species and subspecies have revealed that the closest wild relative of maize is *Z. mays* subsp. *parviglumis*, a native of Central Mexico commonly called Balsas teosinte (Doebley, 1990**a**,**b**; Buckler and Holtsford, 1996; Doebley, 2004). Based on microsatellite data analyses, the ancestor of maize appears to have been initially domesticated from a relatively small population of Balsas teosinte around 9000 years ago (Matsuoka et al., 2002).

These insights into the phylogenetic relationships among the species and subspecies of *Zea* provide a solid foundation necessary for comparative developmental studies of maize and its closest relatives. Most previous studies have focused on morphological development and underlying genetic correlates of many traits associated with plant architecture (Doebley and Stec, 1991; Doebley et al., 1995, 1997; Doust, 2007; Phillips et al., 2009), inflorescences branching (Doebley and Stec, 1991; Vollbrecht et al., 2005; Bortiri et al., 2006; Doust, 2007; Phillips et al., 2009; Gallavotti et al., 2010; Sigmon and Vollbrecht, 2010), and floret development (Galinat, 1985; Sundberg and Orr, 1990; Benz and Iltis, 1992; Dorweiler et al., 1993; Orr and Sundberg, 1994; Sundberg et al., 1995; Dorweiler and Doebley, 1997; Iltis, 2000; Whipple and Schmidt, 2006; Orr and Sundberg, 2007; Weber et al., 2008; Thompson et al., 2009). Recently, a comparative study of Balsas teosinte caryopses (fruit) demonstrated that some cellular features were conserved between maize and its closest relative (Dermastia et al., 2009). Little is known, however, about features associated with the reproductive process such as female gametophyte development, fertilization, and early embryo and en-

dosperm development in the closest wild relative of maize. For instance, the development of the female gametophyte has been studied in only *Z. mays* subsp. *mexicana* (Schrad.) Iltis (Cooper, 1937) (hereafter refer to as Mexicana teosinte); however, this subspecies is not sister (nor putatively ancestral) to maize.

In order to more completely understand the evolution of the developmental features associated with sexual reproduction in maize, additional comparative embryological studies of the closest wild relative, Balsas teosinte, are needed. We studied megasporogenesis, megagametogenesis, and early development of the embryo and endosperm in Balsas teosinte. In addition, the relative timing of reproductive events after pollination, including double fertilization, the first mitotic division of zygote and primary endosperm nucleus, and the cellularization of free nuclear endosperm, were studied to provide an understanding of potentially heterochronic differences in the sexual process between maize and Balsas teosinte.

1.3 Materials and methods

1.3.1 Growth conditions

Seeds of *Zea mays* subsp. *parviglumis* were provided by the U. S. National Plant Germplasm System, Iowa State University, Regional Plant Introduction Station, Ames, Iowa (accession number: Ames 21809; originally collected in Guerrero, Mexico) (USDA, 2012). Seeds were sown in December 2008 and May 2009 in 15-liter plastic pots with Fafard Canadian Growing Mix 2 soil (Conrad Fafard Inc, Miami, USA) in the greenhouse of the Department of Ecology and Evolutionary Biology, University of Colorado at Boulder, U. S. A. Plants were cultivated at 30 °C in daytime and 28 °C at night. When day length was shorter than 16 hours, supplemental lighting (1000 watt Metal Halide lamps) was used to extend day length to 16 hours. Plants were fertilized twice per week with modified Hoaglands solution containing approximately 200 ppm of nitrogen.

1.3.2 Controlled pollination and material collection

Hand pollination was performed from May to June 2009 for plants sown in December 2008, and from October to November 2009 for plants sown in May 2009. To prevent unwanted pollination, some individuals were emasculated and moved to an isolated room and inflorescences bearing female florets were enclosed with a transparent plastic bag when stigmas (silks) began to emerge from the prophylls that enclose the inflorescence. Stigmas elongated continually in the plastic bags before pollen receipt. Since female florets are arranged acropetally along an inflorescence and pollen grains could adhere at any position along a silk, the distance that a pollen tube grew before reaching an ovule varied with the location of the pollen grain on the silk and the position of the floret. In order to reduce the variance in growing distance, one day before hand pollination all of the stigmas of the female florets of an inflorescence were cut back to 1 cm in length beyond the tip of enclosing prophylls (Appendix A.1). Female inflorescences (ears) of emasculated individuals were pollinated at 9 AM with viable pollen grains collected using maize tassel bags (Seedburo Co., IL, USA).

In order to investigate megasporogenesis and megagametogenesis, female inflorescences were collected at various developmental stages before pollination, from early May to late June 2009 for plants sown in December 2008, and from early October to late November 2009 for plants sown in May 2009. To investigate the growth of pollen tubes, pollinated inflorescences were collected at one-hour intervals after pollination, up to twelve hours after pollination. Additional collections were made at 6 and 12 hours as well as one, two and three days after pollination for histological observation.

1.3.3 Histological observation

In order to investigate the development of the female gametophyte and young caryopses, inflorescences and flowers were dissected in 50 mM Pipes buffer (pH 6.8, with 5 mM

EGTA and 1 M $MgSO_4$) under magnification with a Zeiss stereomicroscope STEMI SV 11 (Carl Zeiss, Boerkochen, Germany). Ovaries were fixed in 4% acrolein in a 50 mM Pipes buffer for 24 hours, and then rinsed with a 50 mM Pipes buffer three times. Ovaries were dehydrated through a graded ethanol series, infiltrated and embedded with glycol methacrylate (JB-4 embedding kit; Electron Microscopy Sciences, Hatfield, PA, USA). 4-μm-thick serial sections were obtained using a Leica RM 2155 rotary microtome (Leica Microsystems, Nussloch, Germany) with glass knifes. The ribbons were mounted on slides and stained with 0.1% toluidine blue. Differential interference contrast (DIC) images were taken with a Zeiss Axiophot microscope equipped with a Zeiss Axiocam digital camera that was controlled by Zeiss AxioVision software. Digital adjustments of images included only corrections of brightness, contrast and resolution, processed with Adobe Photoshop CS3 (Adobe Systems, San Jose, CA, USA), and were applied to the entire image except as noted in figure captions.

1.3.4 Pollen tube observations

In order to observe pollen tubes, inflorescences and flowers were fixed in FAA (paraformaldehyde : anhydrous acetic acid : 50% ethanol = 1 : 1: 18) at hourly intervals to twelve HAP. Ovaries with their styles were dissected and hydrated in a graded ethanol series to distilled water. Subsequently, ovaries were immersed in 5% NaOH over night, and then rinsed with distilled water and 50 mM KPO_4. They were stained with 0.01% decolorized aniline blue in 50 mM KPO_4 for 20 minutes (Lausser et al., 2010), and observed under UV using a Zeiss Axiophot epifluorescence microscope.

1.4 Results

1.4.1 Megasporogenesis

In Balsas teosinte, the mature megasporocyte, which is approximately 75 to 100 μm in length and 15 to 25 μm in width, contains abundant small vacuoles and a large nucleus with

a prominent nucleolus and condensed chromosomes (Fig 1.1A). In the 14 ovules we observed at this stage, the nucleus is located in the half of the megasporocyte closest to the micropyle. Subsequently, the megasporocyte undergoes meiosis and forms a linear tetrad of megaspores; a T-shaped arrangement of megaspores was not observed in our study material (N = 4) (Fig 1.1B). The functional megaspore at the chalazal end is larger than the three nonfunctional megaspores (Fig 1.1B). The two megaspores derived from the micropylar dyad begin to degenerate prior to the abortion of the one nonfunctional megaspore from the chalazal dyad (Figs 1.1B, 1.1C). Eventually, all three nonfunctional megaspores completely degenerate, resulting in darkly-staining masses (Fig 1.1D). Thus, the female gametophyte development of Balsas teosinte is monosporic. The functional megaspore is approximately 40 μm long and 14 μm wide (N = 4).

1.4.2 Megagametogenesis

Initiation of the female gametophyte starts with a free nuclear mitotic division in the functional megaspore to form a two-nucleate female gametophyte. One nucleus migrates towards the micropylar end and the other one migrates towards the chalazal end (Fig 1.2A). A central vacuole expands between the two nuclei as they migrate, and a second smaller vacuole (chalazal vacuole) forms and expands between the chalazal nucleus and the chalazal wall of the female gametophyte (Fig 1.2A). Because of differential expansion of the two vacuoles, the shape of the female gametophyte shifts from cylindric to obovate (Fig 1.2B). When the female gametophyte is approximately 80 μm in length, a second round of free nuclear mitoses occurs. The resulting four nuclei are arranged in two pairs, one at the micropylar end of the female gametophyte and the other between the two main vacuoles (Fig 1.2C). These mitotic divisions occur synchronously and perpendicular to each other, and are also nearly perpendicular to the longitudinal axis of the female gametophyte. Subsequently, each pair of nuclei undergoes one more synchronous round of mitotic division, resulting in an eight-nucleate coenocytic female gametophyte (Fig 1.2D). One nucleus of the chalazal

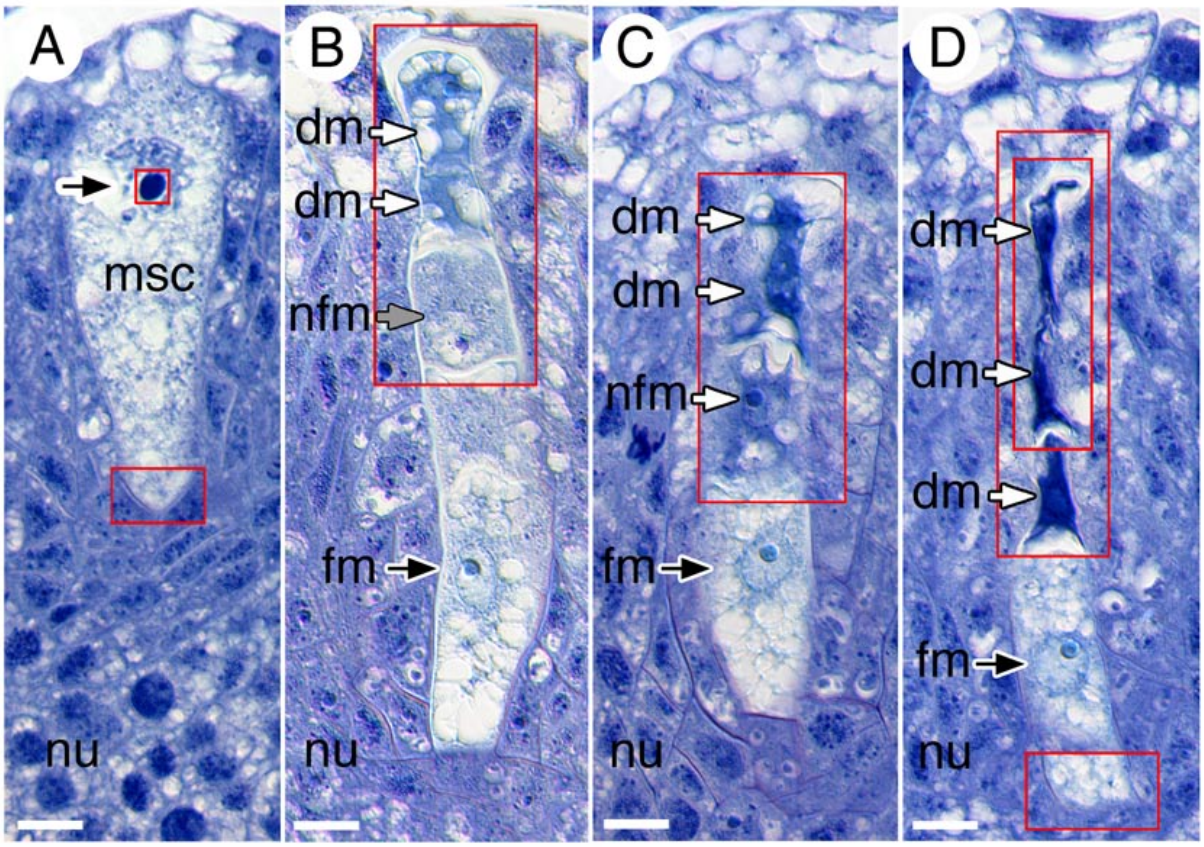

Figure 1.1: **Megasporogenesis in *Zea mays* subsp. *parviglumis*.** All images are oriented so that the micropylar end of the female gametophyte is at the top and the chalazal end is at the bottom. The rectangles indicate the digital superposition of the portion or nucleus from the adjacent histological sections. (A) Megasporocyte containing a conspicuous nucleus with a prominent nucleolus and condensed chromosomes (black arrow). (B) Linear tetrad of megaspores containing a large functional megaspore (black arrow) at the chalazal end. Two megaspores (white arrows) of the micropylar dyad degenerate prior to the abortion of the nonfunctional megaspore (gray arrow) of the chalazal dyad. (C) Functional megaspore (black arrow) with a prominent nucleus and degenerating nonfunctional megaspores (white arrows). (D) Functional megaspore (black arrow) and darkly-stained degenerated megaspores (white arrow). dm, degenerated megaspore; fm, functional megaspore; msc, megasporocyte; nfm, nonfunctional megaspore; nu, nucellus. Bar = 10 μm

quartet (the chalazal polar nucleus) migrates towards the micropylar end and the remaining three nuclei are left at the chalazal end (Fig 1.2D). Cellularization of the eight-nucleate syncytium produces a seven-celled, eight nucleate structure, with three antipodal cells, a central cell with two polar nuclei, and an egg apparatus with two synergids and an egg cell at the micropylar pole of the gametophyte. The two polar nuclei are situated in the peripheral cytoplasm of the central cell adjacent to the egg apparatus (Fig 1.2D).

1.4.3 Maturation of female gametophyte

Following cellularization, the egg apparatus is confined to a relatively small space at the micropylar end of the female gametophyte and starts to differentiate (Fig 1.2E). The egg cell and two synergid cells have nuclei of roughly the same size, but they can be distinguished cytologically as the filiform apparatus starts to differentiate in two synergid cells (Fig 1.2E). Meanwhile, the three antipodal cells that are initially uninucleate begin to undergo a series of asynchronous cell divisions (Fig 1.2E).

While the female gametophyte is expanding, the two synergid cells become highly vacuolate and their nuclei stain lightly. The egg cell also becomes highly vacuolate but the nucleus remains darkly stained (Fig 1.3A). Antipodal cells continue proliferating and their cytoplasm is very dense (Fig 1.3B). In addition, the chalazal vacuole is enclosed by a mass of antipodal cells (Fig 1.3B). As female gametophyte maturation proceeds, the filiform apparatus of each synergid cell becomes dramatically elaborated while their nuclei take on a fusiform shape. The vacuolate egg cell continues to enlarge beyond the size of synergid cells (Fig 1.3C). Starch grains accumulate in the cytoplasm of the egg cell and central cell (Fig 1.3C). The antipodal cells become vacuolate with lightly stained cytoplasm, and some are binucleate (Fig 1.3D). The chalazal vacuole is not distinguishable cytologically at this stage (Fig 1.3D).

When the female gametophyte is fully expanded and mature, the two polar nuclei become partially fused to form a secondary nucleus situated in the marginal cytoplasm of

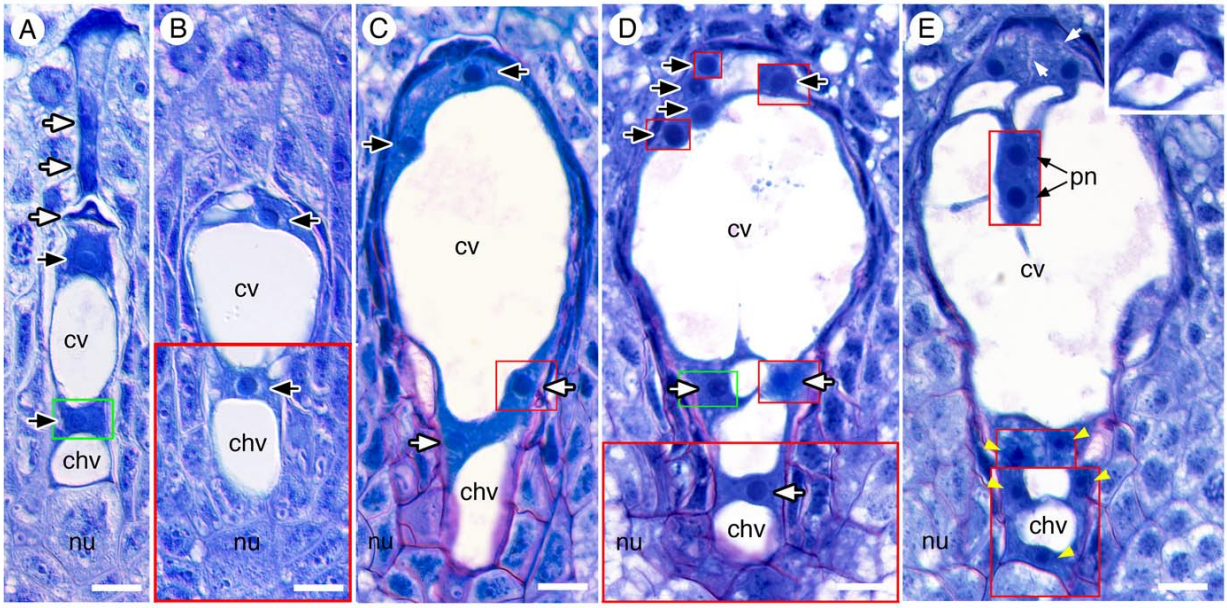

Figure 1.2: **Megagametogenesis in *Zea mays* subsp. *parviglumis***. All images are oriented so that the micropylar end of the female gametophyte is at the top and the chalazal end is at the bottom. The rectangles in red indicate the digital superposition of nuclei from the adjacent histological sections and the rectangles in green indicate the superposition of nuclei from the same section at a different focal point. The inset in **E** shows an egg cell from an adjacent section. (A) Two-nucleate female gametophyte in which the two nuclei (black arrow) are separated by a large central vacuole. A smaller chalazal vacuole is located between the chalazal nucleus and the chalazal wall of the female gametophyte. Degenerated nonfunctional megaspores (white arrows) still visible. (B) Two-nucleate female gametophyte with two nuclei (black arrows). (C) Four-nucleate female gametophyte with a large central vacuole and a small chalazal vacuole. A pair of nuclei (black arrows) is at the micropylar end of the female gametophyte and the other two (white arrows) are in the cytoplasm between a central vacuole and a chalazal vacuole. (D) Eight-nucleate female gametophyte at the initiation of cellularization. Five nuclei (black arrows) are in the micropylar end of the female gametophyte and the other three nuclei (white arrows) are close to the chalazal end. (E) Cellularized ten-nucleate, seven-celled female gametophyte. Egg cell (inset) contains a nucleus and prominent vacuoles while synergids have darkly-stained cytoplasm and smaller vacuoles. Filiform apparatus (white arrows) forms initially in the two synergid cells. Two of three antipodal nuclei have divided, resulting in five antipodal cells (triangles). cv: central vacuole; chv: chalazal-end vacuole; nu: nucellus; pn: polar nucleus. Bar = 10 μm

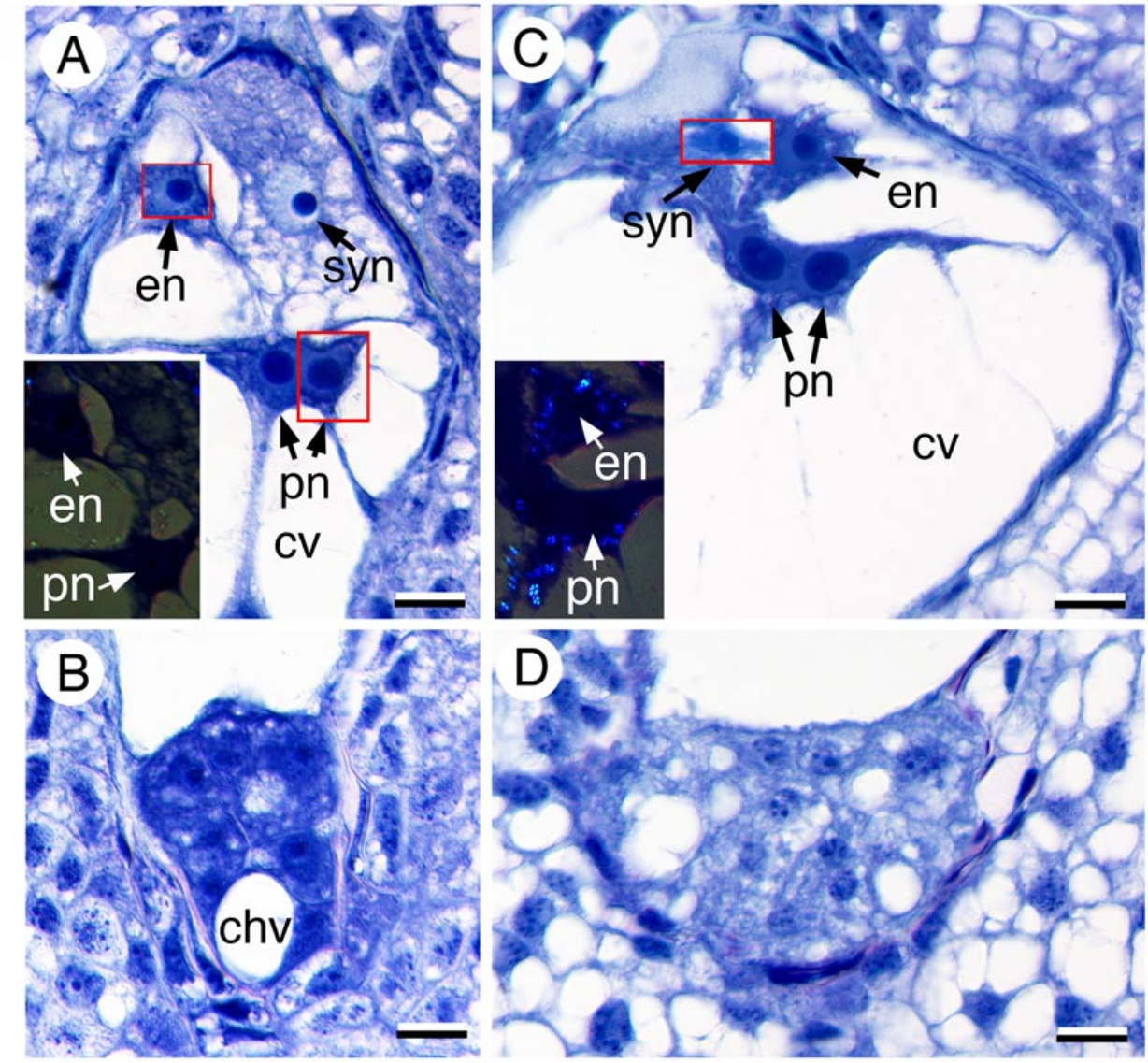

Figure 1.3: **Developmental stages of egg apparatus and antipodal cells during growth of the female gametophyte in *Zea mays* subsp. *parviglumis***. All images are oriented as that micropylar end of the female gametophyte is toward the top and the chalazal end of the female gametophyte is toward the bottom. The rectangles indicate the digital superposition of the portion or nucleus from the adjacent histological sections. The insets in **A** and **C** are images taken with cross-polarization optics to view birefringent starch grains. **A** and **C** showing the histological features of egg apparatus. **B** and **D** showing the histological features of antipodal cells. (A, B) The egg apparatus and antipodal cells during differentiation of the egg apparatus. Inset shows no starch grains in the egg cell and central cell. (C, D) The egg apparatus and antipodal cells prior to the fusion of two polar nuclei. Inset shows starch grains in the egg cell and central cell cytoplasm. cv: central vacuole; chv: chalazal vacuole; en: egg nucleus; pn: polar nucleus; syn: synergid cell nucleus. Bar = 10 μm

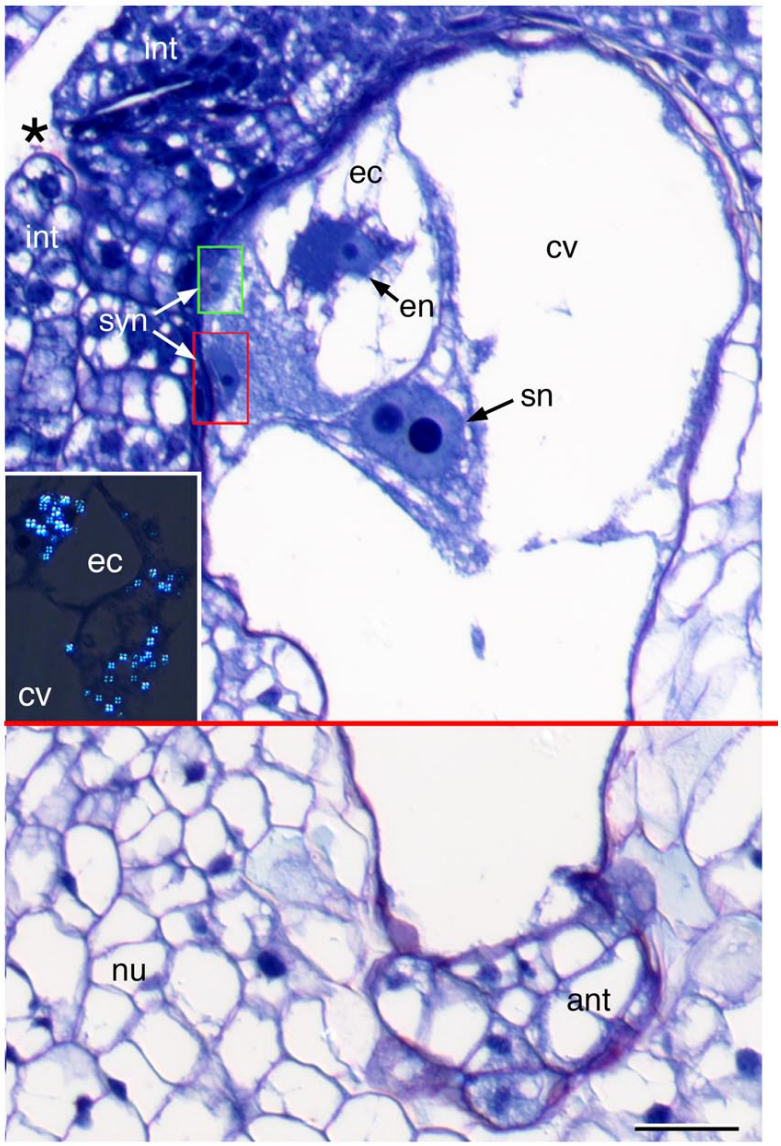

Figure 1.4: **Longitudinal section of a mature female gametophyte in *Zea mays* subsp. *parviglumis***. The image is oriented so that the micropylar end of the female gametophyte is on the top and the chalazal end on the bottom. The rectangle indicates the digital superposition of the portion or nucleus from the adjacent histological sections; horizontal line indicates that there are two sections between the top portion and the bottom portion of the image. The inset shows birefringent starch grains viewed with cross-polarization optics. The central vacuole occupies the majority of a central cell, and cytoplasm is confined to the peripheral region against the wall of a central cell. The egg cell is highly vacuolate and the nucleus is located in the center of the cell. Synergid cell cytoplasm is darkly-stained and the fusiform-shaped nuclei are located adjacent to nucellar cells. Inset shows numerous starch grains in the cytoplasm surrounding the egg nucleus and secondary polar nucleus. Antipodal cells are highly vacuolate. A conspicuous micropyle (black *) formed by inner integuments is right above the micropylar end of the female gametophyte. ant: antipodal cell; cv: central vacuole; ec: egg cell; en: egg nucleus; int: inner integument; nu: nucellus; sn: secondary nucleus; syn: synergids nucleus. Three-dimensional reconstruction of mature female gametophyte is shown in Appendix B.1. Bar = 25 μm

the female gametophyte (Fig 1.4). Additional starch grains accumulate in the peripheral cytoplasm of the central cell, especially around the polar nuclei or secondary nucleus, and in the egg cell (Fig 1.4). At female gametophyte maturity, there may be as many as twenty antipodal cells, most of which are binucleate (Fig 1.4). The last round of mitoses in these cells apparently is not followed by cytokinesis.

1.4.4 Double fertilization and early embryogenesis

Following hand pollination, pollen grains adhere to the stigma papillae and pollen tubes grow on the papilla surface (Fig 1.5A; Appendix A.1C). Pollen tubes penetrate between papilla cells within one hour after pollination (HAP) (Fig 1.5A, Fig 1.7). Subsequently, upon reaching the style, pollen tubes enter the transmitting tract and grow toward the ovary (Fig 1.5A). When pollen tubes arrive at the base of the style they leave the transmitting tract of the style, enter the ovary, and continue to elongate on the surface of the outer and inner integuments to reach the micropyle (Fig 1.5B). In approximately 33% of the observed ovules fixed at six HAP (Table 1.1), a pollen tube had reached the nucellus at the base of the micropyle. The growth rate of pollen tubes can be roughly estimated as 6.5 mm/hour: this represents the longest pollen tube path (39.1 $\pm$ 5.7 mm, n= 35) divided by a duration of six hours to reach the micropyle after pollination.

In approximately 65% of the observed ovules fixed at 12 HAP (Table 1.1), the pollen tube had penetrated the micropylar pole of the female gametophyte and discharged its contents into one of the two synergids (Fig 1.5C). In rare cases, two pollen tubes were observed penetrating the micropylar nucellus of a single ovule, but only one pollen tube delivered its contents, including the two sperm cells, to a synergid cell (Fig 1.5D).

The fertilization of the egg by a sperm and the fusion of the second sperm with the central cell (and its secondary nucleus) occur nearly simultaneously, approximately 12 HAP (Fig 1.6A). The fusion of an egg and a sperm gives rise to a zygote, and the fertilization of the central cell with the other sperm results in the formation of the first endosperm cell

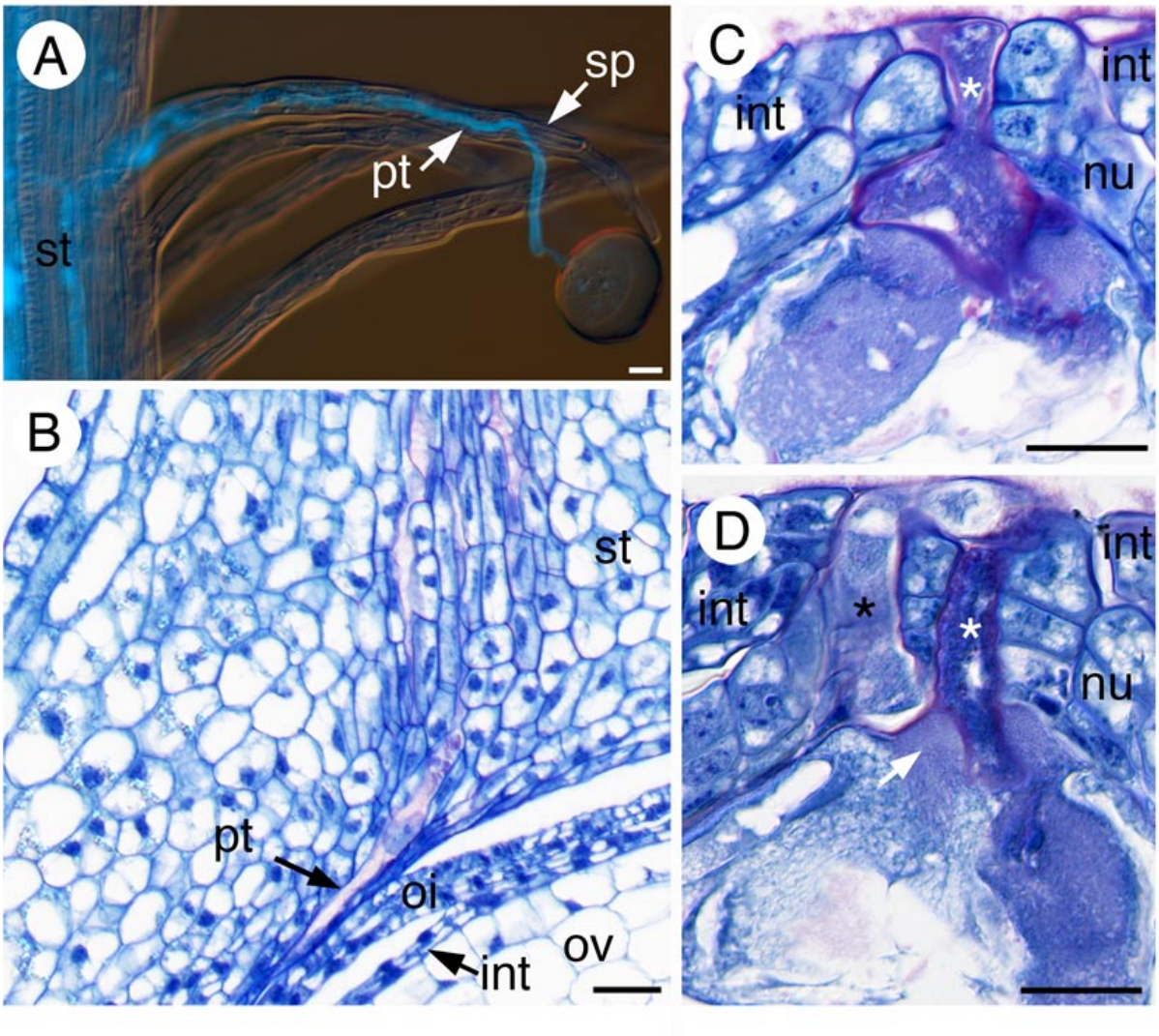

Figure 1.5: **Pollen tube growth in *Zea mays* subsp. *parviglumis***. (A) A pollen tube growing on and in stigmatic papilla. (B) A pollen tube growing in the stylar transmitting tract and on the surface of the outer integument. (C) A pollen tube (white *) penetrating nucellar cells and the micropylar end of the female gametophyte and discharging its content into a synergid cell. (D) Two pollen tubes penetrating the micropylar end of the female gametophyte. One pollen tube (white *) is discharging its content through filiform apparatus (white arrow) in a synergid cell, but the other pollen tube (black *) is intact. int: inner integument; nu: nucellus; oi: outer integument; pt: pollen tube; sp: stigmatic papilla; st: style; ov: ovule. Bar = 20 μm

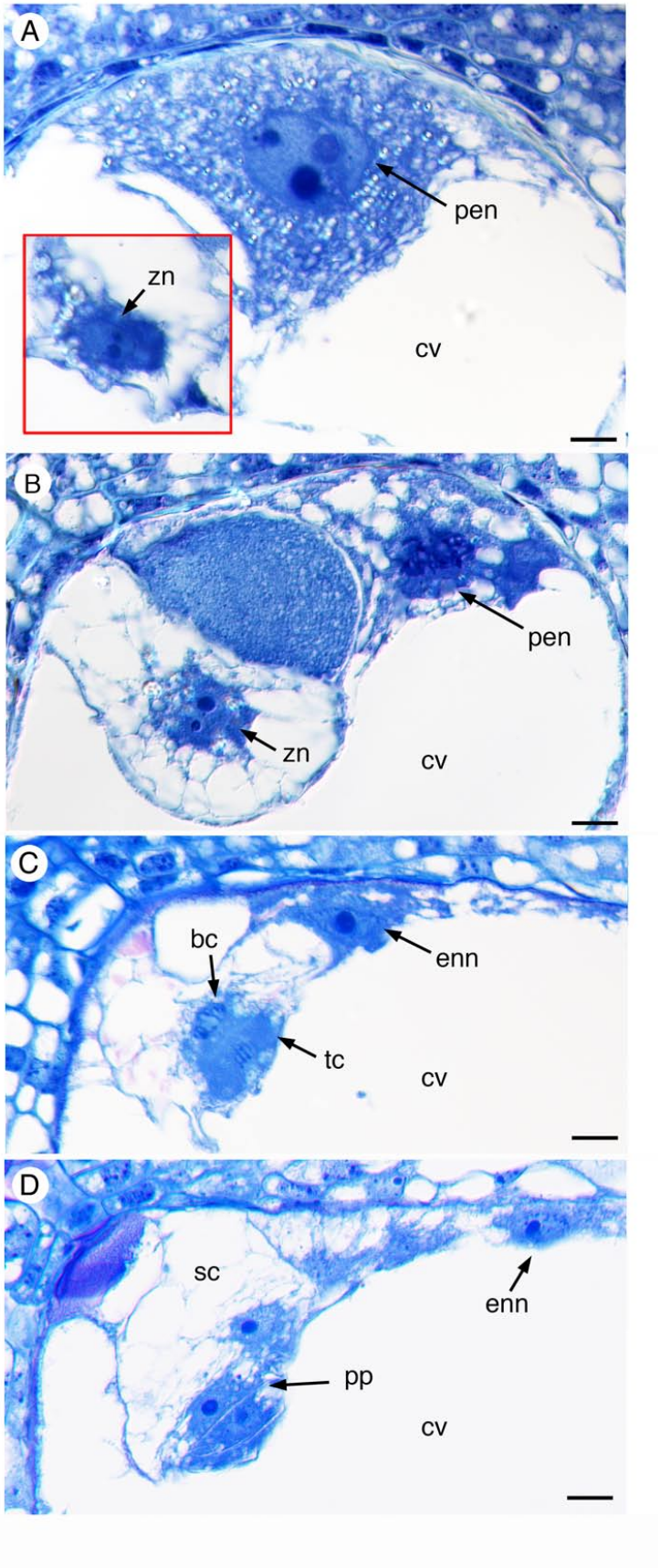

Figure 1.6: **Early embryology in *Zea mays* subsp. *parviglumis*.** (A) The micropylar end of the early developing seed showing a primary endosperm nucleus with three nucleoli, and a zygote with two nucleoli, at twelve hours after controlled pollination. Starch grains are visible around the zygote nucleus and primary endosperm nucleus. (B) The micropylar end of the early developing seed showing a primary endosperm nucleus in the early metaphase and a zygote with two prominent nucleoli at twelve hours after controlled pollination. (C) Early developing seed showing the first mitotic division of the embryo, resulting in a terminal cell and a basal cell one day after controlled pollination. (D) Early developing seed showing a multi-celled embryo two days after controlled pollination. No starch grains are visible in the central cell and early embryo. bc: basal cell; cv: central vacuole; enn: endosperm nucleus; nu: nucellus; pen: primary endosperm nucleus; pp: proembryo proper; sc: suspensor cell; tc: terminal cell; zn: zygote nucleus. Bar = 10 μm

with its primary endosperm nucleus (Fig 1.6A). The primary endosperm nucleus undergoes mitosis to initiate a free nuclear phase of endosperm development whereas the zygote with its single nucleus and two nucleoli had not divided at this point (Fig 1.6).

Approximately 24 HAP, the zygote divides transversely, resulting in a small terminal cell and a large basal cell (Fig 1.6C, 1.7, Table 1.1). At this time, additional free nuclear divisions of the endosperm have produced from four to eight nuclei (or more in few cases) in the peripheral cytoplasm of the single endosperm cell. Forty eight HAP, additional rounds of cell divisions in the embryo have occurred, resulting generally in a two- (or three-) celled embryo proper and a two- (or three-) celled suspensor (Fig 1.6D). The starch grains that had been present in the cytoplasm around the nuclei of the egg and central cell prior to fertilization are not found at this stage (Fig 1.6D). Endosperm in most samples collected 48 HAP was still coenocytic with free nuclei located in the peripheral cytoplasm (Fig 61.6). In 22% of the samples, however, the endosperm had begun to cellularize (Fig 1.7, Table 1.1). Seventy two HAP, endosperm in most samples (83%) is cellularized (Fig 1.7, Table 1.1). Thus, the developmental pattern of endosperm is the nuclear type.

Table 1.1: **Number of samples at each collection time in a particular developmental stage in *Zea mays* subsp. *parviglumis***

Time	Sample size	Event of sexual reproduction						
		No PT in micropyle	PT in micropyle	PT discharged sperm cell	Double fertilization	PE& zygote	FE & embryo	CE & embryo
6 HAP	21	14	7					
12 HAP	14		5	7	1	1		
1 DAP	36	1	2	1	2	31	1	
2 DAP	27	4		2	1	1	13	6
3 DAP	18						3	15

(PT: pollen tube; FE: free nucleate endosperm; CE: cellularized endosperm)

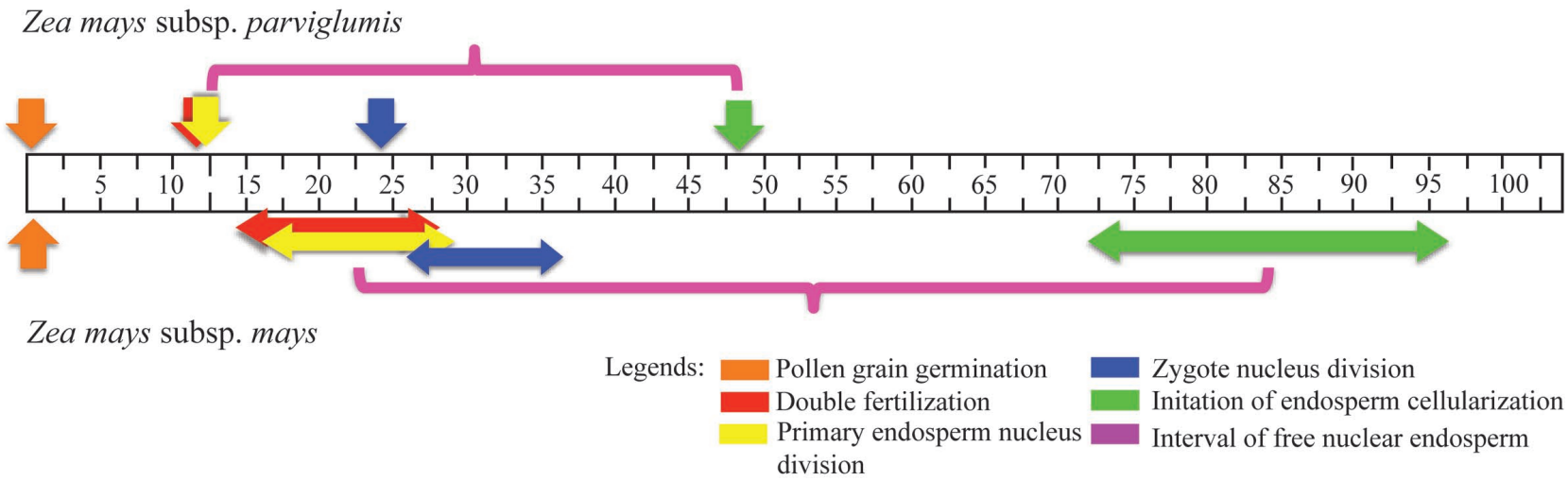

Figure 1.7: **Timing of post-pollination reproductive events of *Zea mays* subsp. *parviglumis* and *Z. mays* subsp. *mays***. Numbers within the scale rectangle indicate the number of hours after controlled pollination. Arrowheads above the scale rectangle indicate the timing of reproductive events in *Z. mays* subsp. *parviglumis*, and the arrowhead and two-headed arrows below the scale rectangle show the range of timing of reproductive events reported for *Z. mays* subsp. *mays*. Brackets indicate the interval of free nuclear endosperm. Data for cultivated maize are summarized from published references listed in Table 1.2 to encompass the most conservative estimate of the timing of each developmental stage. Events occur precociously in *Z. mays* subsp. *parviglumis* compared with *Z. mays* subsp. *mays*. The duration of free nuclear endosperm in *Z. mays* subsp. *parviglumis* (approximately 36 hours) is relatively shorter than that in *Z. mays* subsp. *mays* (approximately 60 hours)

1.5 Discussion

1.5.1 Female gametophyte development

Female gametophyte development in Balsas teosinte is a modification of the Polygonum type, in which the three antipodal cells continue to proliferate after the initial cellularization of the female gametophyte. This modified Polygonum type of female gametophyte development also is found in the sister group of *Zea*, *Tripsacum* (Burson et al., 1990; Leblanc et al., 1995), as well as in other closely related lineages including *Apluda*, *Chionachne*, *Cymbopogon*, *Miscanthus*, and *Sorghum* (Stover, 1937; Choda et al., 1982; Satyamurty, 1984; Bhanwra and Pathak, 1987). A small chalazal vacuole is formed during early megagametogenesis in Balsas teosinte and this characteristic was also found in maize and *Z. mays* subsp. *mexicana* (Cooper, 1937). It is not clear whether or not this developmental feature is common in *Zea*; however, the modified Polygonum type of female gametophyte development likely was present in the common ancestor of species of *Zea mays*.

The number of antipodal cells formed in the Balsas teosinte female gametophyte is about 20. More than 30 antipodal cells have been reported in mature Mexicana teosinte female gametophytes (Cooper 1937; Koul 1959). In maize, the number of antipodal cells usually varies from 20 to 48, although as many as 100 have been reported for some varieties (Hector, 1936; Randolph 1936; Stover 1937; Koul 1959; Diboll and Larson 1966; Diboll 1968; Kiesselbach 1980; Huang and Sheridan, 1994; Evans and Grossniklaus, 2009). In *Tripsacum*, however, four to six antipodal cells are typically formed during female gametophyte development (Burson et al., 1990; Leblanc et al., 1995). The low number of antipodals in the lineage sister to *Zea* suggests that the high levels of antipodal proliferation may have evolved in the common ancestor of *Zea*. Alternatively the lower number of antipodals in *Tripsacum* may be derived rather than plesiomorphic.

More broadly, the number of antipodal cells and nuclei is the most variable characteristic of the female gametophyte in members of the Poaceae, ranging from three, in *Pharus*

lappulaceus (Sajo et al., 2007), *Streptochaeta spicata* (Sajo et al., 2008) and many species in *Eleusine* (Streetman, 1963; Lovisolo and Galati, 2007), to more than 300, in *Sasa paniculata* (Anton and Cocucci, 1984). Developmental lability of antipodal number appears to be a feature of the evolution of Poaceae. Yet, antipodal number is too poorly known for the majority of lineages to reconstruct the evolutionary dynamics of this character in detail. Antipodal cells are thought to function as transfer cells involved in nutrient translocation from the maternal sporophyte to the seed during female gametophyte and/or young seed development (Evans and Grossniklaus, 2009). Antipodal proliferation may be associated with more rapid allocation of resources to the developing embryo nourishing tissue (endosperm).

1.5.2 Progamic starch accumulation

During female gametophyte development starch grains accumulate in the cytoplasm around the egg and central cell nuclei. Following double fertilization, these starch grains diminished completely before initiation of endosperm cellularization. Starch accumulation during the progamic phase of female gametophyte development has been reported in two other subspecies of *Zea*, maize and Mexicana teosinte (Cooper, 1937). Relatively small amounts of starch in the female gametophyte by the time of double fertilization have been reported sporadically for a variety of other taxa (Martin, 1914; Reed, 1924; Smith, 1956; Jensen, 1965; Torosian, 1972; Schulz and Jensen, 1973; Sehgal and Gifford Jr, 1979; Folsom and Peterson, 1984; You and Jensen, 1985; Yan et al., 1991; Kimoto and Tobe, 2001, 2003; Heo et al., 2004; Moco and Mariath, 2004; Lora et al., 2010). It is not clear whether progamic nutrient allocation has evolved independently many times in these disparate angiosperms, or whether it is common and has simply been overlooked by researchers.

1.5.3 Pollen tube growth

Pollen tube growth in maize has been well studied (Adams and Mackay, 1953; Heslop-Harrison et al., 1985; Styles, 1987; Kiesselbach, 1998; Kliwer and Dresselhaus, 2010; Lausser

et al., 2010). Germination of pollen grains and the growth of pollen tubes of Balsas teosinte are generally similar to those of maize. In both taxa, pollen grains germinate on the stigmatic papilla surface, and then pollen tubes grow between papilla cells and transmitting tissue as well as on the surface of integuments toward ovules. When the tips of pollen tubes reach the micropyle of an ovule, typically only one pollen tube penetrates the micropylar end of a female gametophyte and delivers sperm cells into a synergid cell.

In maize, multiple pollen tubes can penetrate an ovule. This can then result in heterofertilization where the two sperm cells participating in double fertilization come from two different pollen tubes (Sprague, 1929, 1932; Kato, 1990, 2001; Kraptchev et al., 2003; Rotarenco and Eder, 2003). In Balsas teosinte, we observed that two pollen tubes occasionally penetrated the micropyle, which suggests that heterofertilization may also occur in this taxon. Genetic studies are needed to determine whether or not heterofertilization actually occurs in Balsas teosinte.

1.5.4 Timing of post-pollination reproductive features of the female gametophyte and young seeds in maize and Balsas teosinte

The particular maize line that most closely resembles the plesiomorphic condition for ovule and seed development in *Zea mays* is unknown. Therefore, we used all of the available published data for maize, grown under a variety of conditions, for comparison with Balsas teosinte (Table 1.2; Fig 1.7). These data should encompass the breadth of timing of the course of developmental events and provide a conservative estimate of the timing of these processes in *Zea mays*. Double fertilization in maize occurs 14 to 28 HAP, the primary endosperm nucleus division occurs 16 to 29 HAP, the first zygote nucleus division occurs 26 to 36 HAP, and the initiation of endosperm cellularization occurs 72 to 96 HAP (Fig 1.7). In general, the timing of reproductive events, including double fertilization, primary endosperm nucleus division, zygote division and free nuclear endosperm cellularization, occur earlier in Balsas teosinte compared to these events in maize (Fig 1.7). The longer time between

pollination and double fertilization in maize (14 to 28 hours compared to 12 hours in Balsas teosinte) is largely due to the greater length of the style through which the pollen tube grows. The distance of pollen tube growth in maize ranges from 10 to 20 cm (Kiesselbach, 1998; Williams, 2008), and this is far greater than the longest growing distance in Balsas teosinte, around 3.91 cm on average in our study. Maize has the greatest pollen tube growth rate reported, ranging from 6.25 mm/hour to 12.5 mm/hour (Williams, 2008). Pollen tube growth rate for Balsas teosinte in our study is within this range, 6.5 mm/hour. Therefore, it is unlikely that differences in pollen tube growth rate explain differences in the timing of fertilization between the subspecies.

The duration of the free nuclear endosperm phase of Balsas teosinte also is shorter than that of maize. The time between primary endosperm nucleus division and initiation of endosperm cellularization is about 36 hours in Balsas teosinte, and is more than approximately 60 hours in maize (Fig 1.7). Interploidy cross experiments in maize (Pennington et al., 2008) and *Arabidopsis thaliana* (Scott et al., 1998; Garcia et al., 2003; Luo et al., 2005; Ohto et al., 2009; Zhou et al., 2009) show that early onset of endosperm cellularization results in small seeds and fruits. We suggest that the longer period of free nuclear endosperm development in maize may be correlated to the characteristic of larger caryopses with more endosperm at maturity, and that this may be related to the direct selection for larger seed/caryopsis size during maize domestication.

Table 1.2: **Timing of developmental events after pollination in *Zea mays* subsp. *mays***

Reproductive event	Time after pollination	Silk length	References
Pollen germination	0.3 hour	N/A	Suen and Huang 2007
Double fertilization	14 hours	11 -14 cm	Mòl et al. 1994
	15 hours	7 - 11 cm	Randolph 1936
	16 hours	3 - 5 cm	Randolph 1936
	16 - 24 hours	N/A	Cooper 1951
	17 hours	11 - 14 cm	Randolph 1936
	23 hours	15 - 18 cm	Randolph 1936
	26 - 28 hours	N/A	Johann 1935
Primary endosperm	16 - 17 hours	11 14 cm	Mòl et al. 1994
nucleus division	19 - 29 hours	N/A	Beoinger and Russell 1994
	26 hours	N/A	Randolph 1936
First zygote division	26 - 36 hours	N/A	Beoinger and Russell 1994
	32 - 36 hours	11 - 14 cm	Mòl et al. 1994
Initiation of endosperm	72 - 96 hours	N/A	Cooper 1951
cellularization	72 hours	N/A	Kowles and Phillips 1988
	72 hours	N/A	Clore et al. 1996
	96 hours	N/A	Randolph 1936

Chapter 2

Kin recognition within a seed: the effect of genetic relatedness of an endosperm to its compatriot embryo on maize seed development

2.1 Abstract

As one of two sexual products resulting from double fertilization in angiosperms, the endosperm nourishes its compatriot embryo during seed development and/or germination and ultimately dies. Previous theoretical studies suggest that the genetic relatedness (coefficient of relatedness) of an endosperm to its embryo in the same seed might determine the amount of resources ultimately available for the embryo during seed development. In this study, we took advantage of the phenomenon of heterofertilization in cultivated maize to empirically test, for the first time, whether genetic relatedness between a diploid embryo and its triploid embryo-nourishing endosperm within a seed impacts the process of resource allocation into and between these two sexually produced entities. We used five genetically distinct maize inbred lines to perform two crossing experiments in the greenhouse and in the field. Dry weights of dissected embryos and endosperms of mature heterofertilized and adjacent homofertilized kernels (fruits) were compared. Embryo weight in heterofertilized kernels was significantly less than that of embryos of homofertilized kernels, while there was no significant difference in endosperm weight between the two types of kernels when controlling for the effects of the paternal genomic background and the pigment marker, R1. Our results suggest that the degree of genetic relatedness of an endosperm to its compatriot embryo affects seed development, and specifically the amount of maternal resources allocated

to an endosperm that are eventually turned over to an embryo within a seed. The lower the coefficient of relatedness of an endosperm to its compatriot embryo, the smaller the embryo. Thus, the endosperm of a heterofertilized seed appears to behave less cooperatively with respect to resource transfer toward its less-closely-related embryo compared to the endosperm of a homofertilized seed.

2.2 Introduction

Angiosperms are characterized by a set of unique reproductive features, including double fertilization, in which two sperm cells from a single male gametophyte (pollen tube) fertilize the egg and the central cell of a female gametophyte (embryo sac) to form an embryo and an endosperm, respectively (Maheshwari, 1950; Davis, 1967; Bhojwani and Bhatnagar, 1978; Johri, 1984; Johri et al., 1992). In the vast majority of angiosperms, the endosperm and embryo are genetically identical except for ploidy (Charnov, 1979; Westoby and Rice, 1982; Queller, 1984, 1989; Friedman, 1995; Friedman et al., 2008; Madrid and Friedman, 2009; Cailleau et al., 2010). The embryo is diploid, but the endosperm is triploid and is composed of one paternal gametophyte genome and two identical maternal gametophyte genomes that are derived from the two polar nuclei in the central cell (Brink and Cooper, 1940, 1947; Maheshwari, 1948; Johri, 1984; Johri et al., 1992; Cailleau et al., 2010). In contrast with the embryo, however, the endosperm does not pass its own genes directly to the next generation. Rather, it is "consumed" by its compatriot embryo during seed development and/or germination (Brink and Cooper, 1940, 1947; Evenari, 1984; Lopes and Larkins, 1993; Costa et al., 2004; Friedman et al., 2008). This nourishing behavior of an endosperm raises a long-standing question: why would the second genetically biparental product of sexual reproduction "sacrifice" itself for the successful function of the embryo (Brink and Cooper, 1940; Charnov, 1979; Westoby and Rice, 1982; Queller, 1983; Friedman, 1995; Friedman et al., 2008)?

Hamilton (1964**a**; 1964**b**) first modeled the evolution of altruistic behavior. His theory

of inclusive fitness showed that altruistic behavior toward relatives can be favored by natural selection when the cost to the altruist is compensated by the benefit to those relatives (discounted by the coefficient of relatedness) (Hamilton, 1964**a**,**b**) . Subsequent theoretical studies extended Hamilton's theory to consider the endosperms and embryos of flowering plants. Many of these analyses focused on the effects of parent-offspring conflict (conflict among sibling embryos for limited resources from the maternal sporophyte) and/or intersexual conflict (conflict between male and female parents over the investment of limited resources in the seeds of a maternal sporophyte) (Charnov, 1979; Cook, 1981; Westoby and Rice, 1982; Queller, 1983, 1984; Law and Cannings, 1984; Mazer, 1987; Haig, 1987; Haig and Westoby, 1988, 1989**a**; Haig, 1990, 2004; Dominguez, 1995; Friedman, 1995; Friedman et al., 2008; Uma Shaanker and Ganeshaiah, 1997; Härdling and Nilsson, 1999, 2001; De Jong et al., 2005; Stewart-Cox et al., 2004). A common thread throughout many of these theoretical analyses of conflict is the relatedness ratio, in which the coefficient of relatedness of an endosperm to its own embryo relative to its relatedness to other embryos on a maternal sporophyte is predicted to affect the relative "aggressiveness"of an endosperm to procure resources from the maternal sporophyte on behalf of its own embryo (Westoby and Rice, 1982; Queller, 1983, 1984; Friedman, 1995; Friedman et al., 2008).

Perhaps more subtle, is the notion of cooperation; that developmental and physiological integrations between an endosperm and its compatriot embryo may be very much dependent on their high degree of genetic relatedness (Charnov, 1979; Willson and Burley, 1983; Friedman, 1995; Friedman et al., 2008). Moreover, because an endosperm is genetically identical (except for gene dosages) to its compatriot embryo, once resources from the maternal sporophyte have been allocated to a seed, the inclusive fitness of an endosperm should be maximized when it works cooperatively to effectively allocate those resources reserves to its compatriot embryo (Friedman, 1995; Friedman et al., 2008).

While the last three decades have produced a rich theoretical literature on conflicts and cooperations among the five kinds of genetic entities involved in angiosperm reproduction

(maternal sporophyte, male gametophyte, female gametophyte, embryo, and endosperm) (Charnov, 1979; Cook, 1981; Queller, 1983, 1984, 1989, 1994; Law and Cannings, 1984; Haig, 1986; Haig and Westoby, 1988, 1989**a**,**b**; Haig, 1990; Härdling and Nilsson, 1999, 2001; Friedman, 1995; Friedman et al., 2008; Baroux et al., 2002; Ma and Sundaresan, 2010; Linkies et al., 2010; Cailleau et al., 2010; Liu et al., 2010; Sundaresan and Alandete-Saez, 2010), there have been few empirical studies [but see Scott et al. (1998) and Pennington et al. (2008)], that test the predictions of the theoretical models of conflict within the seeds of flowering plants. Moreover, prior to this report, no experimental study has ever been designed to examine the expectation that the degree of cooperation between an endosperm and its compatriot embryo within a seed might be correlated with their degree of genetic relatedness.

Here we take the advantage of the naturally occurring phenomenon of heterofertilization in maize (*Zea mays* subsp. *mays*), in which the egg and central cell of a female gametophyte within a single ovule are fertilized by sperm cells from two different pollen tubes (Sprague, 1929, 1932; Robertson, 1984; Gao et al., 2011) to experimentally examine the cooperation between an endosperm and its compatriot embryo in terms of resource allocation. Compared to products of homofertilization, the direct consequence of heterofertilization is to decrease in the coefficient of relatedness of an endosperm to its compatriot embryo, as well as the ratio of an endosperm's genetic relatedness to it own embryo vs. its genetic relatedness to other embryos on the same maternal sporophyte (the relatedness ratio) (Table 2.1). At the same time, the coefficient of relatedness of an endosperm resulting from heterofertilization to embryos in other seeds on a maternal plant is unaltered (Table 2.1). Additionally, the coefficient of relatedness of a maternal sporophyte to an endosperm in a heterofertilized seed does not change relative to endosperms in homofertilized seeds (Table 2.1). In essence, the phenomenon of heterofertilization allowed us to experimentally examine levels of nutritional cooperation between an endosperm and its compatriot embryo within a seed in terms of resource allocation when an endosperm and its compatriot embryo do not share genetically identical (or even closely related) sperm as sires.

Table 2.1: **Coefficient of relatedness between reproductive components and relatedness ratios of monosporic 3N endosperm derived from homofertilization and heterofertilization**

			Origin of paternal genomic contribution through outcrossing				
			Unrelated father			Same father	
Type of fertilization	r^*(En→CEm)	r^*(MS→En)	r^*(MS→Em)	r(En→OEm)	r(En→CEm)/r(En→OEm)	r(En→OEm)	r(En→CEm)/r(En→OEm)
Homofertilization	1	1-*fm*	1-*fm*	2(1-*fm*)/3	3/2(1-*fm*)	[2(1-*fm*)+(1-*fp*)]/3	3/[2(1-*fm*)+(1-*fp*)]
Heterofertilization	2/3	1-*fm*	1-*fm*	2(1-*fm*)/3	1/(1-*fm*)	[2(1-*fm*)+(1-*fp*)]/3	2/[2(1-*fm*)+(1-*fp*)]

(Note: *fm* is the degree of heterozygosity of the maternal sporophyte, and *fp* is the degree of heterozygosity of the paternal sporophyte. *fm* and *fp* is from 0 (completely inbreeding) to 1/2 (random mating). Loci of inbred lines from the the Maize Stock Center, U.S.A. are generally highly homozygous (MaizeGDB; Wright, 1922; Schuler, 1954; Hallauer et al., 2010; M. Sachs, Maize Stock Center, U.S.A. personal communication to CCW); therefore, *fm* and *fp* are essentially 0. Regardless of the origin of paternal genomic contributions through outcrossing (unrelated or related father), the relatedness ratio of endosperm, r(En→CEm) / r(En→OEm), through heterofertilization is always less than that through homofertilization and this is true for any level of *fm* and *fp*. When *fm* and *fp* are zero, the relatedness ratio of the endosperm of homofertilized kernel is 3/2 and that of heterofertilized kernel is 1, if the Endosperm (En) and Other Embryos (OEm) are sired with unrelated pollen donors. The relatedness ratio of endosperm through homofertilization is 1 and that through heterofertilization is 2/3 when the endosperm (En) and other embryos (OEm) are sired with the same pollen donor. Examples are shown in Appendix C. Abbreviations: r, coefficient of relatedness; En, Endosperm; CEm, Compatriot Embryo; OEm, Embryo in Other seeds on the same maternal plant; MS, maternal sporophyte; r(En→CEm) / r(En→OEm), the relatedness ratio which is the ratio of the coefficient of relatedness of an endosperm to its compatriot embryo (CEm) vs. that to embryos (OEm) in other seeds on the same maternal plant under the condition of additive effects of nonimprinted genes (Queller, 1989; Friedman et al., 2008))

Although heterofertilization may be common among flowering plant species, it remains essentially undocumented except in *Z. mays* subsp. *mays*, where the use and study of color markers in kernel formation allow for the direct visualization of embryos and endosperms that have been sired by different pollen tubes (Sprague, 1929, 1932; Robertson, 1984; Gao et al., 2011). We used the R1 allele, which contributes to the production of purple anthocyanin pigments in the endosperm and embryo (Sprague, 1929, 1932; Kato, 1997). In our experimental crosses, a maternal inbred line homozygous for the r1 recessive allele was pollinated with a mixture of pollen from two paternal inbred lines, one of which was homozygous for the R1 allele and the other homozygous for the r1 allele. Fertilization products of the R1 pollen parent will express the anthocyanin pigment, whereas products of the r1 pollen parent will not. Thus, heterofertilized kernels are easily identified because the embryo and endosperm will differ in pigmentation (Sprague, 1929, 1932). We used dry weight as a measure of resource allocation and compared the weight of endosperms and embryos of homofertilized and heterofertilized kernels.

2.3 Materials and methods

2.3.1 Design of crossing experiments

We exploited the infrequent event of heterofertilization in *Z. mays* subsp. *mays* to examine the consequences of changing the basic genetic formula of angiosperm reproduction. To minimize the genetic similarity between an endosperm and its compatriot embryo in a heterofertilized kernel, pedigrees and molecular phylogenetic analyses of maize inbred lines available in the Maize Genetics Cooperation Stock Center, USA (Gerdes and Tracy, 1993; Smith et al., 1985**a**,**b**; Flint-Garcia et al., 2005) were consulted and five inbred lines which are relatively genetically distinct were chosen: B73, X17B, X236M, X17F and W22 (Appendix D). X17F is an L289 variety homozygous for the dominant R1-scm3 allele, in which purple pigment forms in the aleurone layer of the endosperm and the scutellum of the embryo

(MaizeGDB). X236M, a W22 variety, is homozygous for the dominant R1-nj allele, in which purple pigment forms in the distal end (crown) of the aleurone layer of endosperm and in the coleoptile of the scutellum (MaizeGDB). B73, W22 and X17B are homozygous for the r1 recessive allele, which results in no purple pigment in either endosperm or embryo (MaizeGDB).

To control for potential effects of the state of the R1 locus and of paternal genetic background on kernel weight, we used the different lines in two crosses (referred to as the cross A and cross B). B73 was used as the maternal parent in both crosses because it generally has large ears (female inflorescences), typically with more than 300 kernels, and both the R1-nj and R1-smc3 alleles are expressed in the endosperm and embryo of this line when pollinated with pollen carrying these R1 dominant alleles. In cross A, B73 plants were pollinated with a mixture of pollen from X17B (L289 carrying the r1 allele) and X236M (W22 carrying the R1-nj), and in cross B, B73 plants were pollinated with a mixture of pollen from X17F (L289 carrying the R1-scm3 allele) and W22 (carrying the r1 allele) (Appendix D).

2.3.2 Growth conditions

Kernels were provided by the Maize Genetics Cooperation Stock Center at the University of Illinois, Urbana, Illinois (MaizeGDB). A preliminary study using cross A was first performed in summer 2007 in the greenhouses of the Department of Ecology and Evolutionary Biology, University of Colorado, Boulder, USA, and plants were grown in 15-liter plastic pots with Fafard Canadian Growing Mix 2 soil (Conrad Fafard Inc. Miami, USA) under a day length of 16 h and at a temperature of 30 °C during the daytime and 28 °C at night (Plant Transformation Facility, Iowa State University, 2012). During the summers of 2008 and 2009, plants for large-scale pollination experiments of cross A and cross B were grown from seeds in the horticulture field research center of the Department of Horticulture and Landscape Architecture, Colorado State University, Fort Collins, USA. Kernels of both crosses were sowed in May and plants were grown under the normal field conditions.

2.3.3 Controlled pollinations

Crossing experiments were performed by employing standard pollen mixture (Sari-Gorla et al., 1992) and pollination techniques used by maize breeders (University Of Missouri, Columbia). Developing ears (female inflorescences) of B73 were enclosed with ear bags (Seedburo Co., IL, USA) to exclude pollen when the tips of the husks (subtending leaves surrounding an ear) were first visible. On the day before controlled pollination, the tips of the husks and silks (elongating stigmas) were cut off above the tip of the ear, and then re-covered with the bag. The cut silks then grew overnight, and the same length of each silk was exposed beyond the cut husk so that each silk would receive the similar amount of pollen (University Of Missouri, Columbia). On the day of pollination, pollen from an individual tassel (male inflorescence) of paternal individuals was collected using a tassel bag (Seedburo Co., IL, USA) in the morning. Similar volumes of pollen from the two distinct paternal lineages, which are X236M and X17B for cross A and X17F and W22 for cross B, were mixed in an ear bag and then the mixture of pollen was immediately applied to the growing silks of the bagged B73 ears. Pollinated ears were harvested when kernels (fruits) were mature and were dried for weight comparison.

2.3.4 Phenotypic features of kernels

In 2007, 2008 and 2009, a total of 103 fully developed ears were harvested for weight comparisons. Four types of kernels were produced in each of the two crossing experiments (Fig 2.1). In both cross A and cross B, the majority of kernels had an endosperm and an embryo of the same color, either yellow endosperm and yellow embryo (YY) or purple endosperm and purple embryo (PP), indicating that they are almost certainly the products of homofertilization (Fig 2.1). The kernels with a yellow endosperm and purple embryo (YP) or purple endosperm and yellow embryo (PY) are likely the products of heterofertilization (Fig 2.1).

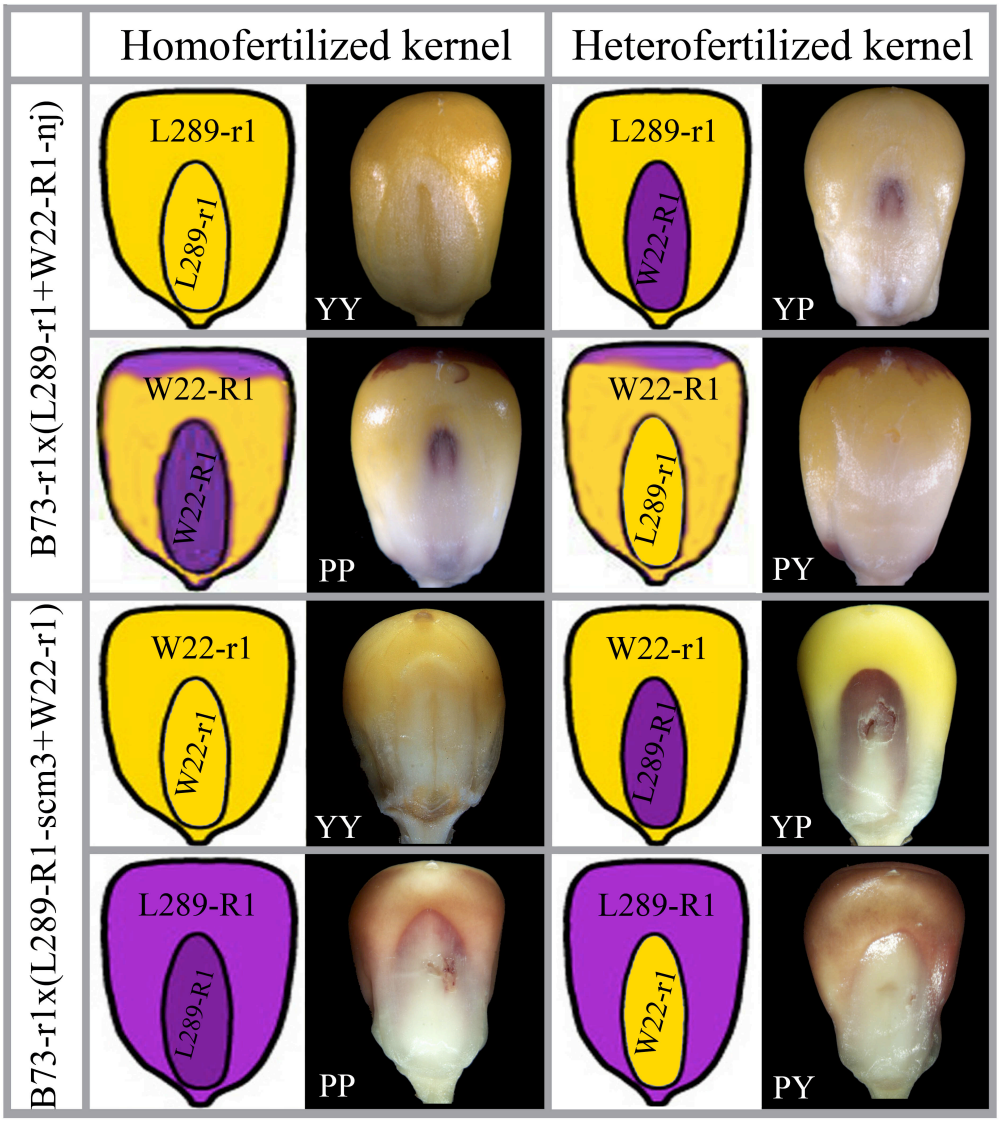

Figure 2.1: **Homofertilized and heterofertilized kernels from cross A (upper four panels) and cross B (lower four panels).** The corresponding cartoons showing paternal genetic background and the state of R1 locus in endosperms and embryos. B73 is the maternal sporophyte for all crosses. The R1 allele of L289 (R1-scm3) creates the purple pigment on the crown of endosperm and embryo, and the R1 allele of W22 (R1-nj) forms a whole purple endosperm or embryo. (YY: yellow endosperm with yellow embryo, PP: purple endosperm with purple embryo, YP: yellow endosperm with purple embryo, PY: purple endosperm with yellow embryo)

2.3.5 Chromosome counts

In both crosses, kernels with a purple endosperm and a yellow embryo (PY) (Fig 2.1) most likely result from heterofertilization (Sprague, 1929, 1932; Kraptchev et al., 2003). However, such kernels could result from a single fertilization event, in which only the central cell of the female gametophyte fuses with a single sperm with the R1 dominant allele while the egg cell with a maternal r1 recessive allele develops into a haploid embryo through parthenogenesis (Kato, 1990, 1997; Kraptchev et al., 2003). A haploid yellow embryo cannot be distinguished from the double recessive embryo visually. Thus we examined chromosome numbers of randomly selected subsamples of these kernels from the 2007 and 2008 crosses. Kernels were germinated in petri dishes, and the distal 5 mm of root tips were cut from 1 week old seedlings and fixed with 2 mM 8-hydroxyquinoline at 15 °C for 2 hours. Root tips were prepared and stained according to Freeling and Malbot (1994), and chromosomes were counted at 1000x magnification. Only kernels with a purple endosperm and a yellow embryo (PY) were examined for chromosome number. Kernels with a yellow endosperm and a purple embryo (YP) must have a diploid embryo since the existence of purple pigment in an embryo indicates that the paternal R1 dominant allele is present in the embryo.

2.3.6 Measurements of embryo and endosperm weight

Kernel location- Because kernel weight varies with its location on a cob, kernel location was included in the analyses of embryo and endosperm weights. Since the phenotype cannot be determined while the kernels are still attached to the cobs (axis of the maize female inflorescence), the kernels were detached and labeled with the number corresponding to that on the reference photographs (Fig 2.2A, 2.2B, Appendix E). Each kernel was then identified as a homofertilized or heterofertilized kernel, and the color of the embryo and endosperm (purple or yellow) was recorded (Fig 2.2D).

Embryo and endosperm weight- For weight comparisons, we selected kernels without

neighboring aborted or abnormal kernels (Fig 2.2A). For each heterofertilized kernel, two adjacent homofertilized kernels, one fertilized by the same pollen parent as the embryo of the heterofertilized kernel and one fertilized by the same pollen parent as the endosperm of the heterofertilized kernel, were selected for weight comparisons (Fig 2.2A, 2.2D). In few cases, the heterofertilized kernel was surrounded by only one kind of homofertilized kernel and then non-adjacent homofertilized kernels at a similar distance from the proximal end of the same cob were randomly selected for weight comparisons.

Kernels were dried at 60 °C for three days and then weighed whole kernels before dissecting the endosperm and the embryo. In order to dissect a kernel, it must first be rehydrated. To prevent kernel germination on rehydration, dried kernels were soaked in FAA (paraformaldehyde: anhydrous acetic acid: 50% alcohol = 1:1:18) for 24 hours. All kernels were hydrated in an ethanol series to distilled water. The kernels were carefully dissected into: pericarp (derived from the ovary wall) plus the residual nucellus, embryo (Fig 2.2C), and endosperm and individually placed into 1.5 ml eppendorf tubes, and were dried at 60 °C for 72 hours. The pericarp plus residual nucellus and the embryo were individually weighed using a digital balance to 0.1 mg (AG 204 Mettler Analytical Balance, Mettler Toledo). Because it was almost impossible to collect all of the endosperm after dissection, the dry weight of endosperm was estimated by subtracting the total dry weight of pericarp plus residual nucellus and embryo from the whole dry kernel weight. We did not consider the weight of the pericarp and residual nucellus in our analysis because it is a part of the maternal sporophyte.

2.3.7 Data analyses

Distribution of heterofertilized kernels- To determine whether the occurrence of heterofertilization was related to the location along an ear, each cob was divided along its axis into four equal sectors, referred to as the first to fourth sector from the distal to proximal end of a cob. Homofertilized kernels and heterofertilized kernels within each sector of each cob were

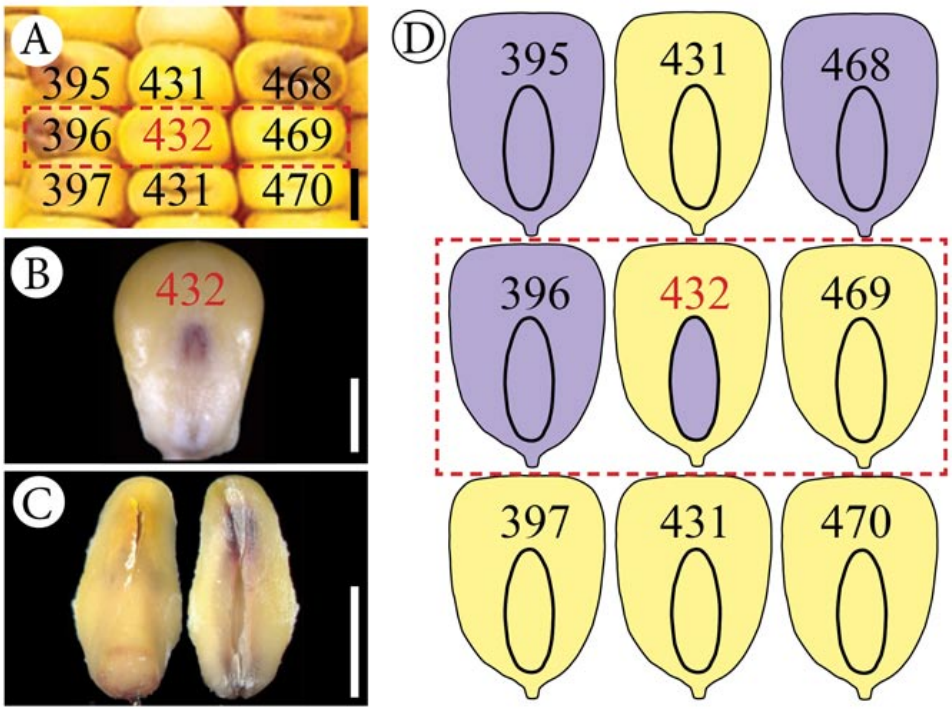

Figure 2.2: **A group of two homofertilized and one heterofertilized kernels as used for weight analyses.** (A) A heterofertilized kernel (labeled with a number in red) surrounded by eight homofertilized kernels (labeled with numbers in black). Red dashed-line rectangle indicates a group of kernels for weight comparisons including a heterofertilized kernel and two adjacent homofertilized kernels. (B) Each kernel from each ear was labeled with a serial number (details in Appendix E). (C) Dissected embryo (the scutellum side on the left and the embryo-axis side on the right). (D) A cartoon showing color phenotypes of endosperms and embryos of kernels in (A). (bar = 5 mm)

counted. The null hypothesis that the frequency of heterofertilized kernels is not different among the four sectors was tested with a chi-square test using the chisq.test function in R version 2.13.0 (R Development Core Team, 2011).

Kernel weight among years- To detect whether kernel weight varied over three years, kernel weight was compared using a one-way ANOVA with year as a fixed effect. Tukey HSD was used for post-hoc pairwise comparison among kernel weight means (Stoline, 1981; Hoaglin et al., 1991). Analyses were performed in the R (R Development Core Team, 2011).

Effect of cross type (A or B) on endosperm and embryo weight- To detect whether weights of endosperm and embryo differed between cross A and cross B, weights of endosperm and embryo were compared using a one-way ANOVA with cross as a fixed effect (Stoline, 1981; Hoaglin et al., 1991).

Correlation of endosperm and embryo weight- To examine the correlation between embryo and endosperm weights across two types of kernels, we used the *cor* function in R (R Development Core Team, 2011).

Effects of fertilization type, paternal genetic background, and the state of the R1 locus on the weight of the whole kernel, embryo, and endosperm- Mixed-effects models (*lme* function from the *nmle* package of R (Pinheiro et al., 2011)) were used to examine the effects of the fertilization type (heterofertilization vs. homofertilization), paternal genetic background (L289 vs. W22), and the state of R1 locus (r1 vs. R1), on kernel, embryo and the endosperm weights. These analyses used planned contrasts to examine the effects of the categorical variables (Appendix F). Because kernel weight varies with its location on a cob, we included the location of kernels (Loc) as a covariate in the mixed-effect models. To aid in interpretation of results, the location of each selected kernel was centered by subtracting the mean location of all selected kernels from the location of the focal kernel (Judd et al., 2008). Each focal heterofertilized kernel (e.g., YP) and two adjacent homofertilized kernels (e.g., one PP and one YY) were considered as a group (Fig 2.2). Fertilization type (FT), paternal genetic background of an embryo (PEm), paternal genetic background of an endosperm

(PEn), state of R1 locus (R), and location of kernel (Loc) were fixed effects, and group, cob, cross, and year were random effects in the analyses. We ran separate models for whole kernel, embryo and endosperm weights. For whole kernel weight, we examined the fixed effects of kernel location (Loc), paternal genetic background of endosperm (PEn), state of R1 locus (R) and their interaction terms. The mixed effect model for embryo weight analysis included fertilization type (FT), paternal genetic background of embryo (PEm), and state of R1 locus (R). For endosperm weight, the mixed effect model included fertilization type (FT), paternal genetic background of endosperm (PEn), and some of their interaction terms. For analyses of the effect of FT on either embryo or endosperm weight, only data from YY and YP kernels (from both cross A and cross B) were included; data from PP kernels were not included because the data from PY kernels were not available for comparison (see results of chromosome counting and Appendix F for contrast codes of FT). Data from PP kernels were included to examine the effects of the other categorical variables, including R, PEm and PEn (see Appendix F for contrast codes). In the mixed effect models for endosperm and embryo weights, only some of all possible interaction terms could be examined because kernels of purple endosperms with yellow embryos (PY) were not included in the data set.

2.4 Results

2.4.1 Chromosome number of yellow embryos

Chromosome numbers of 23 randomly selected PY kernels were examined. Seventeen seedlings were diploid (2N = 20) and likely resulted from heterofertilization (Fig 2.3A). The remaining six seedlings, however, were haploid (N = 10), indicating that the embryos were parthenogenetic (Fig 2.3B). Overall, the frequency of kernels with haploid embryos among kernels with a purple endosperm and a yellow embryo was 23.1%. Because we could not visually distinguish mature kernels containing haploid embryos from those with diploid embryos derived from a heterofertilization event we did not use PY kernels in the weight

analyses.

2.4.2 Frequency and distribution of heterofertilized YP kernel

From 103 ears, there were 40,638 kernels in total, with 9,621, 12,850, 10,995, and 7,172 kernels in the first quarter to fourth quarter of the cob, respectively. 117 (0.29%) kernels had the YP (heterofertilized) phenotype. While the total number of kernels among quarters varied significantly ($\chi^2 = 1688.27$, $p < 0.001$), the frequency of heterofertilized kernels did not vary among quarters ($\chi^2 = 3.00$, $p = 0.3914$). There were 29, 28, 37, and 23 heterofertilized kernels from the first quarter to the fourth quarter, respectively.

2.4.3 Variation of kernel weight among years and between crosses

Of the 117 YP kernels, only 82 had all neighboring kernels fully developed and these were selected for comparisons of embryo and endosperm weight. Each YP kernel along with one adjacent YY kernel and one adjacent PP kernel were designated as a group and used in all subsequent analyses (Fig 2.2A, 2.2D). Mature kernel weight varied significantly among the three years ($F_{(2,243)} = 133.33$, $p < 0.001$). Weights of kernels harvested in the greenhouse in 2007 (Mean ± S.E. = 0.2013 ± 0.0069 g) were greater than that of the kernels harvested from the field in 2008 (Mean ± S.E. = 0.1219 ± 0.0019 g, $p < 0.05$) and 2009 (Mean ± S.E. = 0.1180 ± 0.0020 g, $p < 0.05$). Kernel weights did not differ between 2008 and 2009 ($p = 0.454$).

Means of endosperm and embryo weights in cross B were significantly less than those in cross A (endosperm weight: $F_{(1,244)} = 25.3$, $p < 0.001$; embryo weight: $F_{(1,244)} = 39.48$, $p < 0.001$), except for the mean endosperm weight of paternal L289 background with the R1 dominant allele in cross B (Table 2.2). Additionally, overall, endosperm weight was positively correlated with embryo weight both in homofertilized (YY and PP) and heterofertilized (YP) kernels ($r = 0.91$, $n = 164$, $p < 0.001$ and $r = 0.92$, $n = 82$, $p < 0.001$). There was, however, no significant difference in the coefficient of correlation between two types of kernels ($z =$

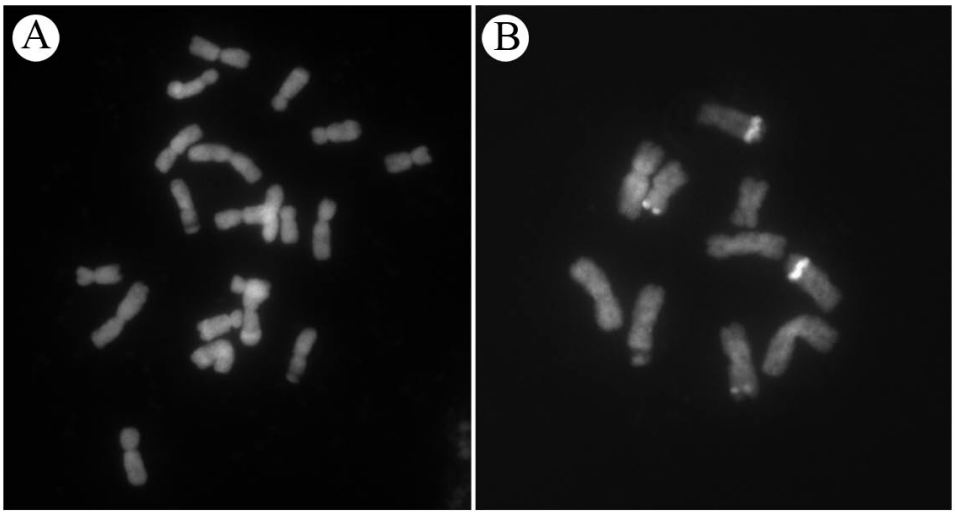

Figure 2.3: **Chromosomes from embryos of kernels with purple endosperm and yellow embryo (PY)**. Embryo of PY is either (A) diploid (2n = 20), or (B) haploid (n = 10).

-0.45, p = 0.65).

2.4.4 Effects of the paternal genetic background and state of R1 locus on kernel weight

The state of the R1 locus had a significant effect on kernel weight (Table 2.3); kernels with the dominant R1 allele were heavier. PEn also significantly affected kernel weight, over and above the effect of the R1 dominant allele (Table 2.3). The mean weight of kernels with endosperm paternal L289 background was greater than kernels with W22 background. There was no interaction between Pen and R1 (Table 2.3). Kernel weight significantly varied depending on the location of the kernel on a cob, and decreased with distance from the proximal end of a cob (Table 2.3). Additionally, the interaction of Loc with R is significant, suggesting that weight of kernels bearing the R1 allele declined with position at a greater rate than those with the recessive allele (Table 2.3). The interaction of PEn with either R or Loc is not significant, however, the three way interaction of Loc, R and PEn was significant. The effect of PEn on kernel weight was greater for when endosperms expressed the R1 allele and were farther from the proximal end of a cob than on kernels that had endosperms with r1 allele and were close to the proximal end of a cob (Table 2.3).

2.4.5 Effects of the fertilization type, paternal genetic background, and state of the R1 locus on embryo and endosperm weight

Only data from YY and YP kernels were compared to test the effect of FT on the weights of the endosperm and embryo. Note that YY and YP kernels were produced in both cross types (A and B) and these kernels include endosperms of the all genetic backgrounds and states of R1 (Fig 2.1). FT significantly affected embryo weight (Table 2.4). The average embryo weight of homofertilized (YY) kernels was greater than that of heterofertilized (YP) kernels. Additionally, embryo weight was significantly associated with the paternal genetic background of the embryo (PEm) (Table 2.4). On average, the weight of an embryo with

Table 2.2: **Means of endosperm and embryo weights (in milligrams)**

Fertilization type	Cross	Paternal genetic background and R1 locus	Endosperm weight (mean±S.E.)	Embryo weight (mean±S.E.)
Homofertilization	A	L289+r1	121.10 ± 6.36	9.383 ± 0.685
	A	W22+R1	121.97 ± 6.35	9.657 ± 0.675
	B	W22+r1	99.51 ± 2.71∗	7.470 ± 0.241∗
	B	L289+R1	106.60 ± 3.05	7.364 ± 0.229∗
Heterofertilization	A	L289+r1	119.40 ± 6.47	N/A
	B	W22+r1	100.25 ± 3.02∗	N/A
	A	W22+R1	N/A	9.586 ± 0.673
	B	L289+R1	N/A	6.881 ± 0.197∗

(Note: $p<0.001$)

the paternal W22 genetic background was greater than an embryo with the L289 genetic background. The interaction of FT and PEm was also significant (Table 2.4); the difference in embryo weight between homofertilized vs. heterofertilized kernels was greater for embryos with the L289 genetic background than embryos with the W22 background. R had no significant effect on embryo weight and no other interactions were significant (Table 2.4).

The effect of FT on endosperm weight was not significant (Table 2.5); mean endosperm weight of homofertilized (YY) kernels was not significantly different from that of heterofertilized (YP) kernels. The paternal genetic background of the endosperm (PEn) significantly affected endosperm weight (Table 2.5). The average weight of an L289 endosperm was greater than that with W22 genetic background. No interactions were significant (Table 2.5).

2.5 Discussion

Endosperm is typically viewed as an entity that behaves cooperatively with, and provides benefits to, its genetically identical compatriot embryo during seed development (Charnov, 1979; Willson and Burley, 1983; Friedman, 1995; Friedman et al., 2008). Furthermore, theoretical models suggest the scenario that the coefficient of relatedness of an endosperm to its compatriot embryo underlies patterns of resource allocation and embryo-nourishing behavior of endosperm (Friedman, 1995; Linkies et al., 2010). By decreasing the genetic relatedness of an endosperm to its compatriot embryo within a kernel, we asked if allocation of resources from the endosperm to its embryo was significantly affected by overall changes in the genetic relatedness associated with heterofertilization. We find that the endosperm of a heterofertilized kernel appears to behave less cooperatively with respect to allocation of resources to its less related embryo compared with the pattern in a homofertilized kernel.

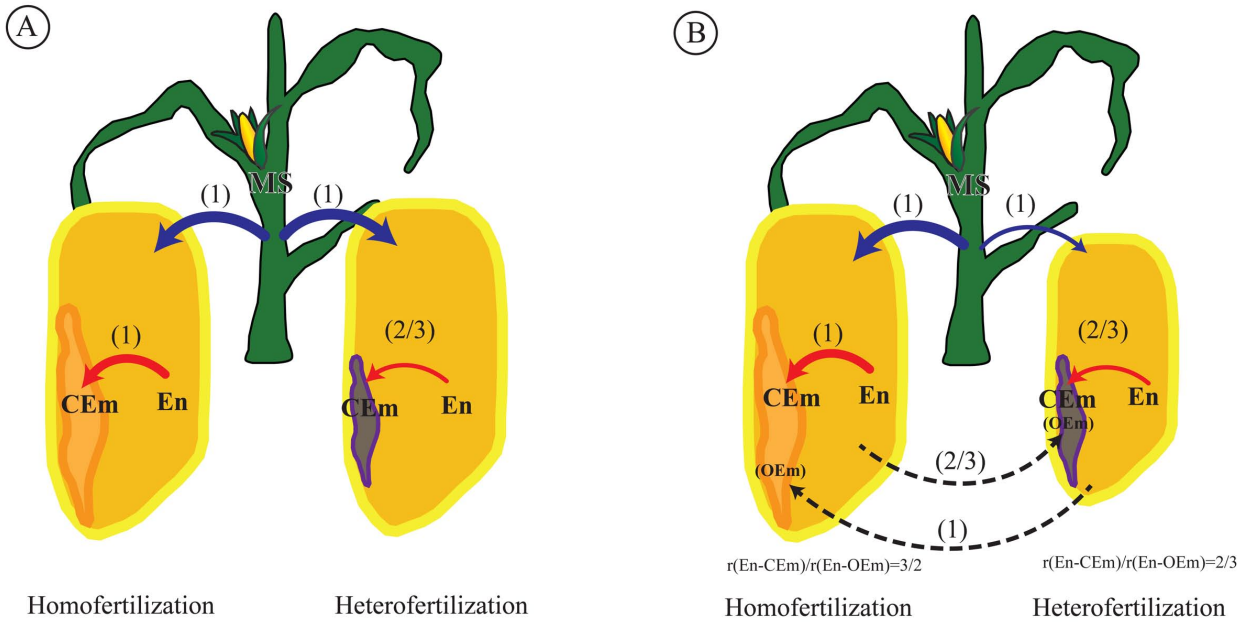

Figure 2.4: **Predicted patterns of resource allocation in homo- and heterofertilized kernels.** (A) Heterofertilization decreases the coefficient of relatedness (r) of embryo and endosperm. If r affects the tendency of endosperm to allocate resources to the embryo, then the embryo of heterofertilized kernels should be smaller than the embryo of homofertilized kernels. The coefficient of relatedness of the maternal sporophyte to the endosperm is not affected. (B) Heterofertilization decreases the relatedness ratio. If this ratio determines the aggressiveness with which an endosperm will garner resources from the maternal sporophyte, then heterofertilized endosperms and kernels should be smaller than those resulting from homofertililzation. Numbers above the arrows indicate the coefficient of relatedness of one identity to the other identity when the parents are highly homozygous (see Table 2.1). Blue arrows indicate transfer from maternal sporophyte to endosperm. Red arrows indicate transfer from endosperm to embryo. Dashed arrows indicate the coefficient of relatedness of an endosperm to an embryo in another kernel. The thickness of arrow line indicates relative amount of resource allocation from one entity to the other entity. Area of endosperm or embryo is related to the size of endosperm or embryo. All parental lines are inbred and assumed homozygous. Color of endosperm or embryo indicates the source of paternal genome.

2.5.1 Frequency of heterofertilization

Two types of heterofertilized kernels were formed: kernels with a yellow endosperm and purple embryo (YP), and kernels with a purple endosperm and yellow embryo (PY) (Fig 2.1). Investigation of chromosome numbers, however, showed that 23.1 % of PY kernels had haploid embryos and were the result of parthenogenesis rather than heterofertilization, that is, only the central cell fused with a sperm cell to form a triploid endosperm (Kato, 1990, 1997, 2001). Because kernels with a yellow diploid embryo cannot be morphologically differentiated from kernels with a yellow haploid embryo, we used only YP kernels to examine the effects of heterofertilization on resource allocation. Assuming that the occurrence of heterofertilized PY kernels was similar to the 0.29 % observed for YP kernels, the overall frequency of heterofertilization in our crosses is approximately 0.58 % (0.29 % x 2). This estimate is consistent with previous reports for the few maize lines that have been examined, in which the frequency of heterofertilization events ranged from 0.5 % to 1 %, and rarely up to 5 % (Sprague, 1932; Sarkar and Coe, 1971; Robertson, 1984; Kraptchev et al., 2003; Rotarenco and Eder, 2003; Yang et al., 2008). The frequency of heterofertilization identifiable by color marker is almost certainly an underestimate because kernels in which an egg and central cell fuse with sperm cells from two different pollen grains with same state of the R1 locus are not morphologically distinguishable from homofertilized kernels. If the frequency of heterofertilization by pollen grains of the same genotype is similar to the frequency of detectable heterofertilization then the actual frequency in our crosses may have been approximately 1 %.

2.5.2 Distribution of heterofertilized kernels on cobs

The occurrence of heterofertilization was independent of kernel position on the cobs, and thus independent of the distance that pollen tubes grow to reach ovules. Although there were more heterofertilized kernels within the second and third quarter of an ear, the

difference in the frequency was not significant and the greater abundance of heterofertilized kernels in the middle portion of the ear was due to the greater number of kernels in two middle quarters of the cob compared to the distal and proximal most quarters. Equal frequency of heterofertilization along the length of the ear is consistent with a previous study using inbred lines with the color inhibitor C^I (Sarkar and Coe, 1971).

2.5.3 Growth condition, paternal genetic background and the R1 dominant allele affect the weight of kernels (including embryo and endosperm)

The mean weight of kernels harvested in the greenhouse (2007) is greater than that of kernels from the field (2008 and 2009). Kernels harvested in the greenhouses were pollinated in early July, and mature kernels were harvested in early November, an approximately three-months grain-filling period under relatively constant conditions, whereas plants growing in the field in 2008 and 2009 had an approximately two-months grain-filling period and experienced low temperature at the end of growing seasons. Kernels weight is significantly affected by the environmental conditions that alter the duration of the grain-filling stage (Blum, 1998; Borrás et al., 2003, 2004; Paponov et al., 2005; Frascaroli et al., 2007; Wang et al., 2007; Gambin et al., 2008). Since the duration of grain-filling stage (deposition of nutrients) is positively correlated with mature kernel weight (Daynard et al., 1971; Daynard and Kannenberg, 1976; Carter and Poneleit, 1973; Cross, 1974; Brooks et al., 1982; Blum, 1998; Gambin et al., 2008), the difference in kernel weight among years is likely due to growing conditions.

Genetic background is well known to affect mature kernel weight in maize (Carter and Poneleit, 1973; Reddy and Daynard, 1983; Tanaka et al., 2009; Hiyane et al., 2010; Severini et al., 2011). Our results clearly show that the two paternal genetic contributions, L289 and W22, had significant, but opposite, effects on the weights of endosperms and embryos (Table 2.4, Table 2.5). The weight of endosperms with L289 paternal genome was greater than the weight of endosperms carrying W22 paternal genome, whereas the embryos with W22

paternal genetic background were larger than the embryos from the L289 paternal origin.

Furthermore, we found that the R1 allele affected kernel weight (Table 2.3). This finding is generally consistent with previous studies showing that the expression of the R gene family results in large kernels (Carter and Poneleit, 1973; Cross, 1979, 1980; Cross and Alexander, 1984; Cross and Dosso, 1989; Cross and Mostafavi, 1994). The effects of R1 locus on embryo and endosperm have never been examined separately. Because the effect of the R1 locus on embryo weight was not significant (Table 2.4), we suggest that increases in kernel weight associated with the R1 locus might be due to changes in endosperm development. The absence of an interaction between Pen and R (Table 2.3) suggests that these two factors act additively, but independently, on mature kernel weight. In summary, differences in resource allocation to kernels are related to the specific genotypes of the parents and/or to the carrier of the R1 color marker. Our crossing design allowed us to control for these factors and isolate the effect of genetic relatedness of embryo and endosperm on resource allocation within the kernels.

2.5.4 Effect of the coefficient of relatedness on the weight of embryos and endosperms

In our crossing experiments of maize inbred lines, the coefficient of relatedness of an endosperm to its compatriot embryo decreases from 1 in homofertilized kernels to 2/3 in heterofertilized kernels (Fig 2.4, Table 2.1). This lower coefficient of relatedness was associated with decreased embryo weight; embryos in heterofertilized kernels were significantly smaller than embryos of adjacent homofertilized kernels. Moreover, this relationship held true even when the effects of PEm, R, and Loc (Table 2.4) were taken into account. Resource transfer from the endosperm to its compatriot embryo during seed development is reduced when the two entities do not share a genetically identical sire. Thus, it would appear that the endosperm in a heterofertilized kernel is less cooperative compared to endosperms in homofertilized kernels (Fig 2.4A). A maternal sporophyte is always equally related to the

endosperms in each of its seeds (Charnov, 1979; Friedman, 1995). Even when heterofertilization occurs, the relatedness of the maternal sporophyte to the endosperm is not altered (assuming that the pollen donors are unrelated to the maternal sporophyte) compared with endosperms in homofertilized kernels (Table 2.1; Fig 2.4A). In our experiments, we detected no significant difference in endosperm weight between homofertilized and heterofertilized kernels, when controlling for position, R1 alleles and paternal genomic background (Table 2.5). This indicates that there is equal allocation of maternal resources to endosperms, irrespective of the relationships of endosperms to their compatriot embryos (Fig 2.4A). The difference in embryo weight between homofertilized and heterofertilized kernels, coupled with no change in endosperm weight, provides a tantalizing hint that the "dialogue "(amount of resource allocation) between an endosperm and maternal sporophyte is not affected by the internal dynamics of the relatedness of an endosperm to its compatriot embryo within an individual seed.

2.5.5 Relatedness ratio is not a predictor of endosperm aggressiveness

The relatedness of an endosperm to its compatriot embryo, relative to its relatedness to other embryos on a maternal sporophyte ("kinship ratio"or "relatedness ratio"), has been viewed as indicative of the degree to which an endosperm should aggressively garner nutrients from the maternal sporophyte (Fig 2.4 B) (Queller, 1983, 1984, 1989; Friedman, 1995; Friedman et al., 2008). The relatedness ratio of an individual is calculated as $r(\text{En}\rightarrow\text{CEm})/r(\text{En}\rightarrow\text{OEm})$, where $r(\text{En}\rightarrow\text{CEm})$ is the relatedness of an endosperm (En) to its compatriot embryo (CEm) and $r(\text{En}\rightarrow\text{OEm})$ is the relatedness of the same endosperm (En) to an embryo in another adjacent seed (other embryo = OEm) on the same maternal sporophyte (Table 2.1, Fig 2.4B). The larger this ratio is, the more aggressively an endosperm is predicted to behave in procuring resources from the maternal sporophyte on behalf of its compatriot embryo within a seed (Westoby and Rice, 1982; Queller, 1983, 1984; Friedman, 1995; Friedman et al., 2008). For inbred maize lines, virtually all loci are homozygous

(Wright, 1922; Schuler, 1954; Hallauer et al., 2010). Therefore, for our crossing experiments in maize, the coefficient of relatedness of a homofertilized endosperm to its compatriot embryo (YY or PP), r(En→CEm), is 1 (Table 2.1). For a heterofertilized endosperm, the coefficient of relatedness to its compatriot embryo (YP or PY), r(En→CEm), is 2/3 (Table 2.1). In addition, because our experimental design used two maize inbred lines as simultaneous pollen sources, the coefficient of relatedness of an endosperm to embryos of adjacent kernels differs depending on the origin of their paternal contributions. For instance, the coefficient of relatedness of an endosperm (e.g., YY) to an embryo in an adjacent kernel with the same father (e.g., YY), r(En→OEm), is 1. The coefficient of relatedness of an endosperm (e.g., YY) to an embryo in an adjacent kernel derived from an unrelated father (e.g., PP), r(En→OEm), is 2/3 (Table 2.1). Thus, the relatedness ratio, r(En→CEm)/r(En→OEm), of an endosperm in a homofertilized kernel to the embryo of an adjacent kernel with the same father (e.g., YY vs. YY), is 1, and to an embryo of an adjacent kernel with an unrelated father (e.g., YY vs. PP) is 3/2 (Table 2.1). In contrast, the relatedness ratio of an endosperm of a heterofertilized kernel to the embryo of an adjacent kernel with the same father (e.g., YP vs. PP) is 2/3, and to an embryo of an adjacent kernel with an unrelated father (e.g., YP vs. YY) is 1 (Table 2.1). Overall, the relatedness ratio for an endosperm derived from heterofertilization is lower than that of an endosperm derived from homofertilization (Table 2.1, Fig 2.4 B). Hence, the endosperm of a homofertilized kernel should favor its compatriot embryo (be more selfish with respect to garnering resources from the maternal sporophyte) at the expense of embryos of neighboring kernels more strongly than endosperms in heterofertilized seeds. Accordingly, inclusive fitness analysis suggests that endosperms in heterofertilized seeds will garner fewer resources from the maternal sporophyte, resulting in a smaller endosperm compared to homofertilized kernels (Fig 2.4 B). Our results, however, show that endosperms of heterofertilized kernels were not significantly smaller than those of adjacent homofertilized kernels (Table 2.5) and provide no support for the hypothesis that the endosperm relatedness ratio influences the aggressiveness of endosperms in procuring

maternal resources in maize.

2.5.6 Fitness of heterofertilized kernels

The lower genetic relatedness of an endosperm to its compatriot embryo in a heterofertilized kernel results in a smaller embryo and comparably-sized endosperm, compared with the sexually formed constituents of a homofertilized kernel. It would be striking to know if the degree of relatedness of an endosperm and embryo truly correlate with the degree of their physiological and developmental cooperation, and ultimately with the fitness of embryos/seedlings that result for heterofertilized and homofertilized seeds. Our data certainly provide an intriguing first set of insights vis á vis embryo size at seed/fruit maturity. But, a legitimate question that remains to be resolved is whether the smaller embryos of heterofertilized kernels are ultimately less fit than the embryos of homofertilization?

Due to the rarity of heterofertilization events and the need to destructively sample all heterofertilized kernels in our experiments for weight analyses, we were not able to examine components of fitness (e.g., germination, growth, and/or survival rates) for embryos of heterofertilized kernels. Seed size is a critical determinant of fitness in many species, affecting germination probability, seedling performance, and survival (Marshall, 1986; Graven and Carter, 1990; Dudley and Lambert, 1992; Nafziger, 1992; Westoby et al., 1992, 1996; Simons and Johnston, 2000; Koelewijn and Van Damme, 2005; Halpern, 2005; Oliver and Borja, 2010). The contribution of embryo size to fitness in these studies is unclear; however, many concerned exalbuminous seeds, for which the embryo is the major component. Based on studies of other species, the smaller embryos of heterofertilized kernels may be less fit than embryos of homofertilized kernels. On the other hand, endosperm weights of heterofertilized and homofertilized kernels are not significantly different and embryos of both kinds of kernels might eventually gain equal access to comparable amounts of stored resources during the germination process. Thus, even though embryos of heterofertilized kernels are relatively smaller at seed/fruit dormancy, these embryos might reach the same developmental

state (dry weight) as embryos of homofertilized kernels by the time the seedlings became fully autotrophic. Even if, the developmental difference detected in dry weight of embryos in heterofertilized and homofertilized seeds at the time of dormancy carry through to the process of seedling establishment the differences in weight may not yield any ultimate fitness consequences. If fitness of heterofertilized embryos is eventually shown not to differ from that of homofertilized embryos, our present results would suggest that the genetic and developmental interactions between endosperm and embryo in maize are significant, but not evolutionarily meaningful. In either case, as tempting as it is to conclude that the degree of cooperation between an endosperm and its compatriot embryo has been shaped by the degree of genetic relatedness and selection, only further (and extremely large and laborious) experiments will be able to conclusively determine this. For now, it is worth noting that we have provided the first tangible data to address the longstanding predictions of inclusive fitness theory and the behaviors and interactions of maternal sporophytes, embryos and endosperms.

2.6 Summary

Within every seed of a flowering plant, five separate genetic and organismic entities interact: the haploid male gametophyte (pollen tube), haploid female gametophyte (embryo sac), diploid maternal sporophyte (integuments and nucellus), diploid embryo, and typically triploid endosperm. Four of these entities (male gametophyte, female gametophyte, embryo and endosperm) also differ genetically between seeds on a single maternal sporophyte. Thus, the remarkable potential for genetic conflict and cooperative behavior has been viewed as likely to occur during the process of reproduction in angiosperms. We exploited the phenomenon of heterofertilization in *Z. mays* subsp. *mays* in which the genetic relatedness of an endosperm to its associated embryo within a kernel was altered and examined the outcome on seed or fruit development. We found a significant effect of genetic relatedness on the cooperative behavior of an endosperm with its own embryo in terms of resource allocation.

While endosperm weight was not significantly different in heterofertilized kernels, compared to homofertilized seeds, embryo weight was significantly less in kernels where the endosperm and embryo were sired by genetically unrelated fathers (heterofertilized kernels). Although we were not able to assess the fitness effects of embryo size, our results support the hypothesis that the cooperation between an endosperm and its compatriot embryo within a kernel is dependent upon the maintenance of close genetic relationship between these two entities.

Table 2.3: **Whole kernel weight.** Mixed effects model analysis of the effects of location (Loc), the state of the R1 locus (R), and paternal genetic background of the endosperm (PEn) on the whole kernel weight, in which results from the type III sums of squares were presented. Regression coefficients indicate slops of sources in the mixed-effect equation. Based on contrast codes we assigned (Appendix F), values of regression coefficients were the half of weight difference between two levels of a source when controlling for the other factors (sources).

Source	Unstandardized regression coefficient ± S.E.	t-value	Pr > |t|
CLo	-0.239 ± 0.0697	-3.43	0.0008∗
R	1.458 ± 0.3641	4.00	0.0001∗
PEn	-2.695 ± 1.3225	-2.04	0.0433∗
R1 x PEn	3.049 ± 2.4633	1.23	0.2176
CLo x R	-0.030 ± 0.0142	-2.13	0.0345∗
CLo x PEn	-0.050 ± 0.0298	-1.68	0.0954
CLo x R x PEn	0.133 ± 0.0469	2.84	0.0052∗

(Note: ∗: $p < 0.05$)

Table 2.4: **Embryo weight.** Mixed effects model analysis of the effects of location (Loc), the type of fertilization (FT), the state of the R1 locus (R), and paternal genetic background of the embryo (PEm) on the embryo weight, in which results from the type III sums of squares were presented. Regression coefficients indicate slops of sources in the mixed-effect equation. Based on contrast codes we assigned (Appendix F), values of regression coefficients were the half of weight difference between two levels of a source when controlling for the other factors (sources).

Source	Unstandardized regression coefficient ± S.E.	t-value	Pr > |t|
CLo	-0.002 ± 0.005	-0.396021	0.6926
FT	0.266 ± 0.111	2.391283	0.0180∗
PEm	0.209 ± 0.055	3.840886	0.0002∗
R	0.174 ± 0.096	1.803612	0.0732
FT x PEm	-0.246 ± 0.106	-2.315604	0.0219∗
CLo x FT	-0.004 ± 0.004	-1.029708	0.3048
CLo x PEm	0.003 ± 0.002	1.404127	0.1623
CLo x R	-0.005 ± 0.004	-1.266750	0.2071
CLo x FT x PEm	-0.005 ± 0.004	-1.346160	0.1802

(Note: ∗: $p < 0.05$)

Table 2.5: **Endosperm weight** Mixed effects model analysis of the effects of location (Loc),type of fertilization (FT), the paternal genetic background of the endosperm (PEn) on the whole kernel weight, in which results from the type III sums of squares were presented. Regression coefficients indicate slops of sources in the mixed-effect equation. Based on contrast codes we assigned (Appendix F), values of regression coefficients were the half of weight difference between two levels of a source when controlling for the other factors (sources).

Source	Unstandardized regression coefficient ± S.E.	t-value	Pr > |t|
CLo	-0.264 ± 0.063	-4.154134	0.0001∗
FT	0.211 ± 0.623	0.338246	0.7356
PEn	-1.589 ± 0.532	-2.985369	0.0033∗
FT x PEn	-0.586 ± 0.623	-0.941453	0.3479
CLo x FT	0.003 ± 0.024	0.119275	0.9052
CLo x PEn	0.004 ± 0.021	0.195194	0.8455
CLo x FT x PEn	0.025 ± 0.024	1.026281	0.3063

(Note: ∗: $p < 0.05$)

Chapter 3

Conclusion

In my dissertation I examined questions related to angiosperm sexual reproduction. By comparing the closest wild subspecies of domesticated maize, Balsas teosinte (*Zea mays* subsp. *parviglumis*), and domesticated maize inbred lines (*Zea mays* subsp. *mays*), I found two significant results. First, I discovered that the duration of the free-nuclear endosperm phase is longer in cultivated maize than in Balsas teosinte. I suggested that this trait could be associated with human selection for bigger seeds with larger endosperm during maize domestication. Second, in maize I empirically demonstrated for the first time the occurrence of kin recognition between an endosperm and its compatriot embryo within a single kernel (fruit), and suggested that the genetic relatedness between these two entities was related to the amount of resource allocated to the embryo in terms of mass. These results not only addressed two fundamental issues related to angiosperm sexual reproduction but also raised some interesting new questions.

In chapter one, I focused on comparisons of the cellular developmental features of the female gametophyte (embryo sac) between domesticated maize and Balsas teosinte and identified sexual reproductive features that might have been altered by selection for bigger seed size during maize domestication and improvement. I found that some features, such as the Polygonum-type-embryo sac with antipodal proliferation and nuclear-type endosperm are conserved between these two subspecies; they are also prevalent throughout the family Poaceae. Despite widespread conservation of a generalized endosperm developmental pat-

tern, there were subtle but important differences between maize and Balsas teosinte. In particular, I identified a difference in the duration of the free nuclear endosperm phase that may be related to seed size. The duration of the free nuclear endosperm phase presumably allows for additional mitotic division of the free endosperm nuclei prior to cellularization in maize compared to Balsas teosinte. These extra mitotic divisions result in more endosperm nuclei before cellularization and consequently may account for greater endosperm content in maize seeds relative to Balsas teosinte.

Within a developing seed, many maternal and paternal genes precisely control resource allocation and endosperm and embryo development (Sabelli and Larkins, 2009; Linkies et al., 2010; He et al., 2011). For example, the Maternally expressed gene1 (Meg1) is responsible for the differentiation of the basal endosperm transfer layer and thus is an important regulator of resource acquisition from the maternal sporophyte, resource partitioning within a seed, and mature seed biomass in maize (Costa et al., 2012). While the development of this transfer layer has already been studied from a traditional developmental point of view in both teosinte and maize (Dermastia et al., 2009), it would be interesting to investigate and compare the spatiotemporal expression patterns of the Meg1 homologous genes in Balsas teosinte and inbred maize lines. Such data will deepen our understanding of the expression of genes associated with the production of larger seeds and endosperm and thus contribute fundamental knowledge for crop improvement.

In chapter two, I experimentally tested the prediction of Hamilton′s inclusive fitness theory for angiosperm sexual reproduction, especially the interaction between an endosperm and its compatriot embryo in terms of resource allocation. By doing crossing experiments, and using endosperm and embryo weights as indicators of resource allocation, I showed that the genetic relatedness of an endosperm to its compatriot embryo has a significant effect on resource allocation, and that the less related the endosperm and embryo in the seed are, the less the endosperm reallocates resources to the embryo during seed maturation. My finding is the first empirical evidence for a long-standing theory of kin selection (recognition) within a

seed. Whereas the question of whether the smaller embryos resulting from heterofertilization are less fit than those resulting from homofertilization remains unknown, our study also raises a fundamental question: what are the cellular and molecular mechanisms for kin recognition between an endosperm and its embryo in plants?

Previous studies of inter-individual recognition in plants largely (though not exclusively) focused on angiosperm reproductive self-incompatibility mechanisms, i.e. how pollen grains (male component) and cells of the stigma and style (female component) interact (Rea and Nasrallah, 2008; Zhang et al., 2009; Higashiyama, 2010; Tantikanjana et al., 2010; McClure et al., 2011). Whether similar "identity "recognition mechanisms have been recruited in the interaction between an endosperm and its compatriot embryo remains unknown. The other potential candidate is a cellular mechanism similar to the major histocompatibility complex (MHC) that has been exclusively found in all vertebrates. The major histocompatibility complex regulars the compatibility among cellular identities, which has been suggested to be partially respect to kin recognition (van Oosterhout, 2009; Martínez-Borra and López-Larrea, 2012). However, the MHC had not been shown in angiosperms. Future studies of endosperm-embryo interactions may reveal a novel mechanism that governs kin recognition and cellular interaction in plants.

Bibliography

Adams, J. D., and E. Mackay. 1953. Observing pollen tubes within the styles of *Zea mays* L. Stain Technology 28:295–298.

Anton, A. M., and A. E. Cocucci. 1984. The grass megagametophyte and its possible phylogenetic implications. Plant Systematics and Evolution 146:117–121.

Baroux, C., C. Spillane, and U. Grossniklaus. 2002. Evolutionary origins of the endosperm in flowering plants. Genome Biology 3:1026.1–1026.5.

Benz, B. F., and H. H. Iltis. 1992. Evolution of female sexuality in the maize ear (*Zea mays* L. subsp. *mays* - Gramineae). Economic Botany 46:212–222.

Beoinger, P., and S. D. Russell. 1994. Gametogenesis in maize, pages 48–64. Springer Verlag.

Bhanwra, R. K., and P. Pathak. 1987. Embryology of *Apluda mutica* (Poaceae). Proceedings: Plant Sciences 97:461–467.

Bhojwani, S. S., and S. P. Bhatnagar. 1978. The embryology of angiosperms. Vikas Publishing House Pvt. Ltd., New Delhi.

Blum, A. 1998. Improving wheat grain filling under stress by stem reserve mobilisation. Euphytica 100:77–83.

Borrás, L., G. A. Slafer, and M. E. Otegui. 2004. Seed dry weight response to source–sink manipulations in wheat, maize and soybean: a quantitative reappraisal. Field Crops Research 86:131–146.

Borrás, L., M. E. Westgate, and M. E. Otegui. 2003. Control of kernel weight and kernel water relations by postflowering source–sink ratio in maize. Annals of Botany 91:857–867.

Bortiri, E., G. Chuck, E. Vollbrecht, T. Rocheford, R. Martienssen, and S. Hake. 2006. *ramosa2* encodes a LATERAL ORGAN BOUNDARY domain protein that determines the fate of stem cells in branch meristems of maize. Plant Cell 18:574–585.

Brink, R. A., and D. C. Cooper. 1940. Double fertilization and development of the seed in angiosperms. Botanical Gazette 102:1–25.

———. 1947. The endosperm in seed development. Botanical Review 13:423–477.

Brooks, A., C. F. Jenner, and D. Aspinall. 1982. Effects of water deficit on endosperm starch granules and on grain physiology of wheat and barley. Functional Plant Biology 9:423–436.

Buckler, E. S., and T. P. Holtsford. 1996. *Zea* systematics: ribosomal ITS evidence. Molecular Biology Evolution 13:612–622.

Burson, B. L., P. W. Voigt, R. A. Sherman, and C. L. Dewald. 1990. Apomixis and sexuality in eastern gamagrass. Crop Science 30:86–89.

Cailleau, A., P.-O. O. Cheptou, and T. Lenormand. 2010. Ploidy and the evolution of endosperm of flowering plants. Genetics 184:439–453.

Carter, M., and M. Poneleit. 1973. Black layer maturity and filling period variation among inbred lines of corn (*Zea mays* L.). Crop Science 13:436–439.

Charnov, E. L. 1979. Simultaneous hermaphroditism and sexual selection. The Proceedings of the National Academy of Sciences USA 76:2480–2484.

Choda, S. P., H. Mitter, and R. K. Bhanwra. 1982. Embryological studies in three species of *Cymbopogon* Spreng (Poaceae). Proceedings: Plant Sciences 91:55–60.

Clore, A. M., J. M. Dannenhoffer, and B. A. Larkins. 1996. EF-1α is associated with a cytoskeletal network surrounding protein bodies in maize endosperm cells. The Plant Cell 8:2003–2014.

Cook, R. E. 1981. Plant parenthood. Natural history 90:30–32.

Cooper, D. C. 1937. Macrosporogenesis and embryo-sac development in *Euchlaena mexicana* and *Zea mays*. Journal of Agricultural Research 55:539–551.

———. 1951. Caryopsis development following matings between diploid and tetraploid strains of *Zea mays*. American Journal of Botany 38:702–708.

Costa, L. M., J. F. Gutièrrez-Marcos, and H. G. Dickinson. 2004. More than a yolk: the short life and complex times of the plant endosperm. Trends in Plant Science 9:507–514.

Costa, L. M., J. Yuan, J. Rouster, W. Paul, H. Dickinson, and J. F. Gutierrez-Marcos. 2012. Maternal control of nutrient allocation in plant seeds by genomic imprinting. Current Biology 22:160–165.

Cross, H. 1974. Diallel analysis of duration and rate of grain filling of seven inbred lines of corn. Crop Science 15:532–535.

———. 1979. Yield responses to selection for variable R-nj expression in early maize. Crop Science 20:411–412.

———. 1980. Use of R-nj aleurone color to improve grain yields of early maize. Crop Science 21:751–754.

Cross, H. Z., and W. L. Alexander. 1984. Effects of parents and planting dates on R-nj expression in maize. Euphytica 33:577–582.

Cross, H. Z., and H. Dosso. 1989. R-nj aleurone color selection and grain-filling responses in opaque-2 maize. Euphytica 43:269–274.

Cross, H. Z., and M. R. Mostafavi. 1994. Grain filling of R-nj color-selected maize strains divergently selected for kernel weight. Canadian journal of plant science 74:455–460.

Davis, G. L. 1967. Systematic embryology of the angiosperms. John Wiley & Sons., New York.

Daynard, T. B., and L. W. Kannenberg. 1976. Relationships between length of the actual and effective grain filling periods and the grain yield of corn. Canadian Journal of Plant Science 56:237–242.

Daynard, T. B., J. W. Tanner, and W. G. Duncan. 1971. Duration of the grain filling period and its relation to grain yield in corn (*Zea mays* l.). Crop Science 11:45–48.

De Jong, T. J., H. Van Dijk, and P. G. L. Klinkhamer. 2005. Hamilton's rule, imprinting and parent-offspring conflict over seed mass in partially selfing plants. Journal of Evolutionary Biology 18:676–682.

Dermastia, M., A. Kladnik, J. Dolenc Koce, and P. S. Chourey. 2009. A cellular study of teosinte *Zea mays* subsp. *parviglumis* (Poaceae) caryopsis development showing several processes conserved in maize. American Journal of Botany 96:1798–1807.

Doebley, J. 1990a. Molecular evidence and the evolution of maize. Economic Botany 44:6–27.

———. 1990b. Molecular systematics of *Zea* (Gramineae). Maydica 35:143–150.

———. 2003. The taxonomy of *Zea*. {http://teosinte.wisc.edu/taxonomy.html accessed on Feb 25, 2012}.

———. 2004. The genetics of maize evolution. Annual Review of Genetics 38:37–59.

Doebley, J., and H. Iltis. 1980. Taxonomy of *Zea* (Gramineae). I. A subgeneric classification with key to taxa. American Journal of Botany 67:982–993.

Doebley, J., and A. Stec. 1991. Genetic analysis of the morphological differences between maize and teosinte. Genetics 129:285–295.

Doebley, J., A. Stec, and C. Gustus. 1995. *teosinte branched1* and the origin of maize: evidence for epistasis and the evolution of dominance. Genetics 141:333–346.

Doebley, J., A. Stec, and L. Hubbard. 1997. The evolution of apical dominance in maize. Nature 386:485–488.

Dominguez, C. A. 1995. Genetic conflicts of interest in plants. Trends in Ecology and Evolution 10:412–416.

Dorweiler, J., A. Stec, J. Kermicle, and J. Doebley. 1993. *Teosinte glume architecture 1*: A genetic locus controlling a key step in maize evolution. Science 262:233–235.

Dorweiler, J. E., and J. Doebley. 1997. Developmental analysis of *teosinte glume architecture1*: a key locus in the evolution of maize (Poaceae). American Journal of Botany 84:1313–1322.

Doust, A. 2007. Architectural evolution and its implications for domestication in grasses. Annals of Botany 100:941–950.

Dudley, J. W., and R. J. Lambert. 1992. Ninety generations of selection for oil and protein in maize. Maydica 37:1–7.

Evans, M. M. S., and U. Grossniklaus. 2009. The Maize Megagametophyte, chap. 4, pages 79–104. Springer.

Evenari, M. 1984. Seed physiology: from ovule to maturing seed. Botanical Review 50:143–170.

Flint-Garcia, S. A., A.-C. C. Thuillet, J. Yu, G. Pressoir, S. M. Romero, S. E. Mitchell, J. Doebley, S. Kresovich, M. M. Goodman, and E. S. Buckler. 2005. Maize association population: a high-resolution platform for quantitative trait locus dissection. Plant Journal 44:1054–1064.

Folsom, M. W., and C. M. Peterson. 1984. Ultrastructural aspects of the mature embryo sac of soybean, *Glycine max* (L.) Merr. Botanical Gazette 145:1–10.

Frascaroli, E., M. A. Canè, P. Landi, G. Pea, L. Gianfranceschi, M. Villa, M. Morgante, and M. E. Pè. 2007. Classical genetic and quantitative trait loci analyses of heterosis in a maize hybrid between two elite inbred lines. Genetics 176:625–644.

Freeling, M., and V. Walbot. 1994. The Maize handbook. Springer-Verlag, New York.

Friedman, W. E. 1995. Organismal duplication, inclusive fitness theory, and altruism: understanding the evolution of endosperm and the angiosperm reproductive syndrome. Proceedings of the National Academy of Sciences of USA 92:3913–3917.

Friedman, W. E., E. N. Madrid, and J. H. Williams. 2008. Origin of the fittest and survival of the fittest: relating female gametophyte development to endosperm genetics. International Journal of Plant Sciences 169:79–92.

Galinat, W. C. 1985. The missing links between teosinte and maize: A review. Maydica 30:137–160.

Gallavotti, A., J. A. Long, S. Stanfield, X. A. Yang, D. Jackson, E. Vollbrecht, and R. J. Schmidt. 2010. The control of axillary meristem fate in the maize *ramosa* pathway. Development 137:2849–2856.

Gambin, B. L., L. Borras, and M. E. Otegui. 2008. Kernel weight dependence upon plant growth at different grain-filling stages in maize and sorghum. Australian Journal of Agricultural Research 59:280–290.

Gao, S., R. Babu, Y. Lu, C. Martinez, Z. Hao, A. F. Krivanek, J. Wang, T. Rong, J. Crouch, and Y. Xu. 2011. Revisiting the hetero-fertilization phenomenon in maize. PloS one 6:232–244.

Garcia, D., V. Saingery, P. Chambrier, U. Mayer, G. Jürgens, and F. Berger. 2003. Arabidopsis *haiku* mutants reveal new controls of seed size by endosperm. Plant Physiology 131:1661–1670.

Gerdes, J. T., and W. F. Tracy. 1993. Pedigree diversity within the lancaster surecrop heterotic group of maize. Crop Science 33:334–337.

Graven, L. M. C., and P. R. Carter. 1990. Seed size/shape and tillage system effect on corn growth and grain yield. J. Prod. Agric 3:445–452.

Haig, D. 1986. Conflicts among megaspores. Journal of theoretical biology 123:471–480.

———. 1987. Kin conflict in seed plants. Trends in Ecology and Evolution 2:337–340.

———. 1990. New perspectives on the angiosperm female gametophyte. The Botanical Review 56:236–274.

———. 2004. Genomic imprinting and kinship: how good is the evidence? Annual Review Genetics 38:553–585.

Haig, D., and M. Westoby. 1988. Inclusive fitness, seed resources, and maternal care, chap. 3, pages 60–79. Oxford University Press, New York.

———. 1989a. Parent-specific gene expression and the triploid endosperm. American Naturalist 134:147–155.

———. 1989b. Selective forces in the emergence of the seed habit. Biological Journal of the Linnean Society 38:215–238.

Hallauer, A. R., M. J. Carena, and J. B. Miranda Filho. 2010. Quantitative genetics in maize breeding. 3rd ed. Springer, New York ; London.

Halpern, S. 2005. Sources and consequences of seed size variation in lupinus perennis (fabaceae): adaptive and non-adaptive hypotheses. American Journal of Botany 92:205–213.

Hamilton, W. D. 1964a. The genetical evolution of social behaviour. I. Journal of Theoretical Biology 7:1–16.

———. 1964b. The genetical evolution of social behaviour. II. Journal of Theoretical Biology 7:17–52.

Härdling, R., and P. Nilsson. 1999. Parent-offspring and sexual conflicts in the evolution of angiosperm seeds. Oikos 84:27–34.

———. 2001. A model of triploid endosperm evolution driven by parent-offspring conflict. Oikos 92:417–423.

He, G., A. A. Elling, and X. W. Deng. 2011. The epigenome and plant development. Annual Review Plant Biology 62:411–435.

Heo, K., Y. Kimoto, M. Riveros, and H. Tobe. 2004. Embryology of Gomortegaceae (Laurales): characteristics and character evolution. Journal of Plant Research 117:221–228.

Heslop-Harrison, Y., J. Heslop-Harrison, and B. J. Reger. 1985. The pollen-stigma interaction in the grasses, 7: pollen-tube guidance and the regulation of tube number in *Zea mays*. Acta Botanica Neerlandica (Netherlands) 34:193–211.

Higashiyama, T. 2010. Peptide signaling in pollen–pistil interactions. Plant and cell physiology 51:177–189.

Hiyane, R., S. Hiyane, A. C. Tang, and J. S. Boyer. 2010. Sucrose feeding reverses shade-induced kernel losses in maize. Annals of Botany 106:395–403.

Hoaglin, D. C., F. Mosteller, and J. W. Tukey. 1991. Fundamentals of exploratory analysis of variance. Wiley Series in Probability and Statistics. John Wiley and Sons, Inc.

Iltis, H. H. 2000. Homeotic sexual translocations and the origin of maize (*Zea mays*, Poaceae): A new look at an old problem. Economic Botany 54:7–42.

Iltis, H. H., and B. F. Benz. 2000. *Zea nicaraguensis* (Poaceae), a new teosinte from Pacific Coastal Nicaragua. Novon 10:382–390.

Iltis, H. H., and J. F. Doebley. 1980. Taxonomy of *Zea* (Gramineae). II. Subspecific categories in the *Zea mays* complex and a generic synopsis. American Journal of Botany 67:994–1004.

Jensen, W. A. 1965. The ultrastructure and composition of the egg and central cell of cotton. American Journal of Botany 52:781–797.

Johann, H. 1935. Histology of the caryopsis of yellow dent corn, with reference to resistance and susceptibility to kernel rots. Journal of Agricultural Research 51:855–883.

Johri, B., K. Ambegaokar, and P. Srivastava. 1992. Comparative embryology of angiosperms, vol. 1. illustrated ed. Springer-Verlag, New York.

Johri, B. M. 1984. Embryology of angiosperms. Springer-Verlag, Berlin.

Judd, C. M., G. H. McClelland, and C. S. Ryan. 2008. Data analysis : a model comparison approach. 2nd ed. Routledge, New York ; Hove.

Kato, A. 1990. Heterofertilization exhibited by using highly haploid inducing line "Stock 6" and supplementary cross. Maize Genet Coop Newslett 64:109–110.

———. 1997. Induced single fertilization in maize. Sexual Plant Reproduction 10:96–100.

———. 2001. Heterofertilization exhibited by trifluralin-induced bicellular pollen on diploid and tetraploid maize crosses. Genome 44:1114–1121.

Kiesselbach, T. A. 1998. The structure and reproduction of corn. 2nd ed. CSHL Press, Cold Spring Harbor, N.Y.

Kimoto, Y., and H. Tobe. 2001. Embryology of Laurales: a review and perspectives. Journal of Plant Research 114:247–267.

———. 2003. Embryology of Siparunaceae (Laurales): characteristics and character evolution. Journal of Plant Research 116:281–294.

Kliwer, I., and T. Dresselhaus. 2010. Establishment of the male germline and sperm cell movement during pollen germination and tube growth in maize. Plant Signaling and Behavior 5:885–889.

Koelewijn, H. P., and J. M. M. Van Damme. 2005. Effects of seed size, inbreeding and maternal sex on offspring fitness in gynodioecious plantago coronopus. Journal of Ecology 93:373–383.

Kowles, R. V., and R. L. Phillips. 1988. Endosperm development in maize. International Review of Cytology 112:97–136.

Kraptchev, B., M. Kruleva, and T. Dankov. 2003. Induced heterofertilization in maize (*Zea mays* L.). Maydica 48:271–274.

Kremer, J. R., D. N. Mastronarde, and J. R. McIntosh. 1996. Computer visualization of three-dimensional image data using imod. Journal of Structural Biology 116:71–76.

Lausser, A., I. Kliwer, K.-O. O. Srilunchang, and T. Dresselhaus. 2010. Sporophytic control of pollen tube growth and guidance in maize. Journal of Experimental Botany 61:673–682.

Law, R., and C. Cannings. 1984. Genetic analysis of conflicts arising during development of seeds in the Angiospermophyta. Proceedings of the Royal Society of London. Series B, Biological Sciences 221:53–70.

Leblanc, O., M. D. Peel, J. G. Carman, and Y. Savidan. 1995. Megasporogenesis and megagametogenesis in several *Tripsacum* species (Poaceae). American Journal of Botany 82:57–63.

Linkies, A., K. Graeber, C. Knight, and G. Leubner-Metzger. 2010. The evolution of seeds. New Phytologist 186:817–831.

Liu, Y., Z. Q. Yan, N. Chen, X. T. Di, J. J. Huang, and G. Q. Guo. 2010. Development and function of central cell in angiosperm female gametophyte. Genesis 48:466–478.

Lopes, M. A., and B. A. Larkins. 1993. Endosperm origin, development, and function. Plant Cell 5:1383–1399.

Lora, J., J. I. Hormaza, and M. Herrero. 2010. The progamic phase of an early-divergent angiosperm, *Annona cherimola* (Annonaceae). Annals of Botany 105:221–231.

Lovisolo, M. R., and B. G. Galati. 2007. Ultrastructure and development of the megagametophyte in *Eleusine tristachya* (Lam.) Lam. (Poaceae). Flora 202:293–301.

Luo, M., E. S. Dennis, F. Berger, W. J. Peacock, and A. Chaudhury. 2005. *MINISEED3* (*MINI3*), a *WRKY* family gene, and *HAIKU2* (*IKU2*), a leucine-rich repeat (*LRR*) *KINASE* gene, are regulators of seed size in *Arabidopsis*. Proceedings of the National Academy of Science of USA 102:17531–17536.

Ma, H., and V. Sundaresan. 2010. Development of flowering plant gametophytes. Current Topics in Developmental Biology 91:379–412.

Madrid, E. N., and W. E. Friedman. 2009. The developmental basis of an evolutionary diversification of female gametophyte structure in *Piper* and Piperaceae. Annals of Botany 103:869–884.

Maheshwari, P. 1948. The angiosperm embryo sac. The Botanical Review 14:1–56.

———. 1950. An introduction to the embryology of angiosperms. McGraw-Hill, New York.

MaizeGDB. 2012. Maize genetics and genomics database {http://www.maizegdb.org/ accessed on Feb 25, 2012}.

Marshall, D. L. 1986. Effect of seed size on seedling success in three species of sesbania (fabaceae). American Journal of Botany pages 457–464.

Martin, J. N. 1914. Comparative morphology of some Leguminosae. Botanical Gazette 58:154–167.

Martínez-Borra, J., and C. López-Larrea. 2012. The emergence of the major histocompatibility complex. Self and Nonself pages 277–289.

Matsuoka, Y., Y. Vigouroux, M. M. Goodman, J. Sanchez G, E. Buckler, and J. Doebley. 2002. A single domestication for maize shown by multilocus microsatellite genotyping. Proceedings of the National Academy of Science of USA 99:6080–6084.

Mazer, S. J. 1987. Maternal investment and male reproductive success in angiosperms: parent-offspring conflict or sexual selection? Biological Journal of the Linnean Society 30:115–133.

McClure, B., F. Cruz-García, and C. Romero. 2011. Compatibility and incompatibility in s-rnase-based systems. Annals of botany 108:647–658.

Moco, M. C. C., and J. E. A. Mariath. 2004. Female gametophyte development in *Adesmia latifolia* (Spreng.) Vog (Leguminosae-Papilionoideae). Revista Brasileira de Botanica 27:241–248.

Mòl, R., E. Matthys-Rochon, and C. Dumas. 1994. The kinetics of cytological events during double fertilization in *Zea mays* L. The Plant Journal 5:197–206.

Nafziger, E. D. 1992. Seed size effects on yields of two corn hybrids. Journal of production agriculture 5:538–540.

Ohto, M.-A. A., S. K. Floyd, R. L. Fischer, R. B. Goldberg, and J. J. Harada. 2009. Effects of APETALA2 on embryo, endosperm, and seed coat development determine seed size in *Arabidopsis*. Sexual Plant Reproduction 22:277–289.

Oliver, P. A. T., and M. E. L. Borja. 2010. Seed mass variation, germination time and seedling performance in a population of pinus nigra subsp salzamannii. FOREST SYSTEMS 3:DEC 2010.

Orr, A. R., and M. D. Sundberg. 1994. Inflorescence development in a perennial teosinte: *Zea perennis* (Poaceae). American Journal of Botany 81:598–608.

———. 2007. Inflorescence development in the teosinte *Zea luxurians* (Poaceae) and implication for the origin of maize inflorescences. Maydica 52:31–47.

Paponov, I. A., P. Sambo, G. S. Erley, T. Presterl, H. H. Geiger, and C. Engels. 2005. Grain yield and kernel weight of two maize genotypes differing in nitrogen use efficiency at various levels of nitrogen and carbohydrate availability during flowering and grain filling. Plant and Soil 272:111–123.

Pennington, P. D., L. M. Costa, J. F. Gutierrez-Marcos, A. J. Greenland, and H. G. Dickinson. 2008. When genomes collide: aberrant seed development following maize interploidy crosses. Annals of Botany 101:833–843.

Phillips, K. A., A. L. Skirpan, N. J. Kaplinsky, and P. McSteen. 2009. *Developmental disaster1*: A novel mutation causing defects during vegetative and inflorescence development in maize (*Zea mays*, Poaceae). American Journal of Botany 96:420–430.

Pinheiro, J., D. Bates, S. DebRoy, D. Sarkar, and R. D. C. Team. 2011. Package 'nlme'.

Plant Transformation Facility, Iowa State University. 2012. Greenhouse care for transgenic maize plants.

Queller, D. C. 1983. Kin selection and conflict in seed maturation. Journal of Theoretical Biology 100:153–172.

———. 1984. Models of kin selection on seed provisioning. Heredity 53:151–165.

———. 1989. Inclusive fitness in a nutshell. Oxford surveys in evolutionary biology 6:73–109.

———. 1994. Male-female conflict and parent-offspring conflict. The American Naturalist 144:84–99.

R Development Core Team. 2011. R: A Language and Environment for Statistical Computing. R Foundation for Statistical Computing, Vienna, Austria.

Randolph, L. F. 1936. Developmental morphology of the caryopsis in maize. Journal of Agricultural Research 53:881–916.

Rea, A. C., and J. B. Nasrallah. 2008. Self-incompatibility systems: barriers to self-fertilization in flowering plants. Int J Dev Biol 52:627–636.

Reddy, V., and T. Daynard. 1983. Endosperm characteristics associated with rate of grain-filling and kernel size in corn. Maydica 28:339–355.

Reed, E. L. 1924. Anatomy, embryology, and ecology of *Arachis hypogea*. Botanical Gazette 78:289–310.

Robertson, D. S. 1984. A study of heterofertilization in diverse lines of maize. Journal of Heredity 75:457–462.

Rotarenco, V., and J. Eder. 2003. Possible effects of heterofertilization on the induction of maternal haploids in maize. Maize Genetics Cooperation Newsletter 77:30.

Sabelli, P. A., and B. A. Larkins. 2009. The development of endosperm in grasses. Plant Physiol 149:14–26.

Sajo, M. G., H. Longhi-Wagner, and P. J. Rudall. 2007. Floral development and embryology in the early-divergent grass *Pharus*. International Journal of Plant Sciences 168:181–191.

Sajo, M. G., H. M. Longhi-Wagner, and P. J. Rudall. 2008. Reproductive morphology of the early-divergent grass *Streptochaeta* and its bearing on the homologies of the grass spikelet. Plant Systematics and Evolution 275:245–255.

Sari-Gorla, M., M. E. Pe, D. L. Mulcahy, and E. Ottaviano. 1992. Genetic dissection of pollen competitive ability in maize. Heredity 69:423–423.

Sarkar, K. R., and E. H. Coe. 1971. Analysis of events leading to heterofertilization in maize. Journal of Heredity 62:118–120.

Satyamurty, T. V. C. 1984. Development of the caryopsis in *Chionachne koenigii* Linn. Plant Sciences 93:567–570.

Schuler, J. F. 1954. Natural mutations in inbred lines of maize and their heterotic effect. I. Comparison of parent, mutant and their F1 hybrid in a highly inbred background. Genetics 39:908–922.

Schulz, P., and W. A. Jensen. 1973. *Capsella* embryogenesis: the central cell. Journal of Cell Science 12:741–763.

Scott, R. J., M. Spielman, J. Bailey, and H. G. Dickinson. 1998. Parent-of-origin effects on seed development in *Arabidopsis thaliana*. Development 125:3329–3341.

Sehgal, C. B., and E. M. Gifford Jr. 1979. Developmental and histochemical studies of the ovules of *Nicotiana rustica* L. Botanical Gazette 140:180–188.

Severini, A. D., L. Borras, M. E. Westgate, and A. G. Cirilo. 2011. Kernel number and kernel weight determination in dent and popcorn maize. Field Crops Research 120:360–369.

Sigmon, B., and E. Vollbrecht. 2010. Evidence of selection at the *ramosa1* locus during maize domestication. Molecular Ecology 19:1296–1311.

Simons, A. M., and M. O. Johnston. 2000. Variation in seed traits of lobelia inflata (campanulaceae): sources and fitness consequences. American Journal of Botany 87:124–132.

Smith, B. W. 1956. *Arachis hypogaea*. normal megasporogenesis and syngamy with occasional single fertilization. American Journal of Botany 43:81–89.

Smith, J. S. C., M. M. Goodman, and C. W. Stuber. 1985a. Genetic variability within US maize germplasm. I. Historically important lines. Crop Science 25:550–555.

———. 1985b. Genetic variability within US maize germplasm. II. Widely-used inbred lines 1970 to 1979. Crop Science 25:681–685.

Sprague, G. F. 1929. Hetero-fertilization in maize. Science 69:526–527.

———. 1932. The nature and extent of hetero-fertilization in maize. Genetics 17:358–368.

Stewart-Cox, J. A., N. F. Britton, and M. Mogie. 2004. Endosperm triploidy has a selective advantage during ongoing parental conflict by imprinting. Proceedings of the Royal Society of London series B-Biological Sciences 271:1737–1743.

Stoline, M. R. 1981. The status of multiple comparisons: simultaneous estimation of all pairwise comparisons in one-way ANOVA designs. American Statistician 35:134–141.

Stover, E. L. 1937. The embryo sac of *Eragrostis cilianensis* (All.) Link. Ohio Journal of Science 37:172–184.

Streetman, L. J. 1963. Reproduction of the lovegrasses, the genus *Eragrostis* - I.E. Chloromelas Steud., *E. curvula* (Schrad.) Nees, E. Lehmanniana Nees, and *E. superba* Peyr. Wrightia 3:41–51.

Styles, E. 1987. Pollen tube growth in maize. Maydica 32:139–150.

Suen, D. F., and A. H. C. Huang. 2007. Maize pollen coat xylanase facilitates pollen tube penetration into silk during sexual reproduction. Journal of Biological Chemistry 282:625–636.

Sundaresan, V., and M. Alandete-Saez. 2010. Pattern formation in miniature: the female gametophyte of flowering plants. Development 137:179–189.

Sundberg, M. D., C. LaFargue, and A. R. Orr. 1995. Inflorescence development in the "standard exotic" maize, argentine popcorn (Poaceae). American Journal of Botany 82:64–74.

Sundberg, M. D., and A. R. Orr. 1990. Inflorescence development in two annual teosintes: *Zea mays* subsp. *mexicana* and *Z. mays* subsp. *parviglumis*. American Journal of Botany 77:141–152.

Tanaka, W., A. I. Mantese, and G. A. Maddonni. 2009. Pollen source effects on growth of kernel structures and embryo chemical compounds in maize. Annals of Botany 104:325–334.

Tantikanjana, T., M. E. Nasrallah, and J. B. Nasrallah. 2010. Complex networks of self-incompatibility signaling in the brassicaceae. Current opinion in plant biology 13:520–526.

Thompson, B. E., L. Bartling, C. Whipple, D. H. Hall, H. Sakai, R. Schmidt, and S. Hake. 2009. *bearded-ear* encodes a MADS box transcription factor critical for maize floral development. Plant Cell 21:2578–2590.

Torosian, C. E. D. 1972. Ultrastructural and histochemical studies of endosperm differentiation in *Lobelia dunnii*. Ph.D. thesis. University of California, Berkeley.

Uma Shaanker, R., and K. N. Ganeshaiah. 1997. Conflict between parent and offspring in plants: predictions, processes and evolutionary consequences. Current Science- Bangalore 72:932–939.

University Of Missouri, Columbia. 2012. Controlled pollinations of maize. {http://www.maizegdb.org/IMP/WEB/pollen.htm; accessed on Feb. 25, 2012}.

USDA. 2012. Ames 21809: *Zea mays* subsp. *parviglumis* H. H. Iltis & Doebley. {http://www.ars-grin.gov/cgi-bin/npgs/acc/display.pl?1087195; accessed on Feb. 25, 2012}.

van Oosterhout, C. 2009. A new theory of mhc evolution: beyond selection on the immune genes. Proc Biol Sci 276:657–65.

Vollbrecht, E., P. S. Springer, L. Goh, E. S. Buckler, and R. Martienssen. 2005. Architecture of floral branch systems in maize and related grasses. Nature 436:1119–1126.

Wang, X., H. Cao, D. Zhang, B. Li, Y. He, J. Li, and S. Wang. 2007. Relationship between differential gene expression and heterosis during ear development in maize (*Zea mays* L.). Journal of Genetics and Genomics 34:160–170.

Weber, A. L., W. H. Briggs, J. Rucker, B. M. Baltazar, J. de Jesús Sánchez-Gonzalez, P. Feng, E. S. Buckler, and J. Doebley. 2008. The genetic architecture of complex traits in teosinte (*Zea mays* ssp. *parviglumis*): new evidence from association mapping. Genetics 180:1221–1232.

Westoby, M., E. Jurado, and M. Leishman. 1992. Comparative evolutionary ecology of seed size. Trends in Ecology & Evolution 7:368–372.

Westoby, M., M. Leishman, J. Lord, H. Poorter, and D. J. . J. Schoen. 1996. Comparative ecology of seed size and dispersal [and discussion]. Philosophical Transactions of the Royal Society B: Biological Sciences 351:1309–1318.

Westoby, M., and B. Rice. 1982. Evolution of the seed plants and inclusive fitness of plant tissues. Evolution 36:713–724.

Whipple, C. J., and R. J. Schmidt. 2006. Genetics of grass flower development. Advances in Botanical Research: Incorporating Advances in Plant Pathology 44:385–424.

Williams, J. H. 2008. Novelties of the flowering plant pollen tube underlie diversification of a key life history stage. Proceedings of the National Academy of Sciences of USA 105:11259–11263.

Willson, M. F., and N. Burley. 1983. Mate choice in plants: tactics, mechanisms, and consequences, vol. 19. Princeton University Press.

Wright, S. 1922. Coefficients of inbreeding and relationship. The American Naturalist 56:330–338.

Yan, H., H. Y. Yang, and W. A. Jensen. 1991. Ultrastructure of the developing embryo sac of sunflower (*Helianthus annuus*) before and after fertilization. Canadian Journal of Botany 69:191–202.

Yang, W., Y. Zheng, and J. Wu. 2008. Heterofertilization of the *opaque-2* endosperm in maize. Hereditas 145:225–230.

You, R., and W. A. Jensen. 1985. Ultrastructural observations of the mature megagametophyte and the fertilization in wheat (*Triticum aestivum*). Canadian Journal of Botany 63:163–178.

Zhang, Y., Z. Zhao, and Y. Xue. 2009. Roles of proteolysis in plant self-incompatibility. Annual review of plant biology 60:21–42.

Zhou, Y., X. Zhang, X. Kang, X. Zhao, X. Zhang, and M. Ni. 2009. SHORT HYPOCOTYL UNDER BLUE1 associates with *MINISEED3* and *HAIKU2* promoters in vivo to regulate *Arabidopsis* seed development. Plant Cell 21:106–117.

Appendix A

Female inflorescence of mature Balsas teosinte

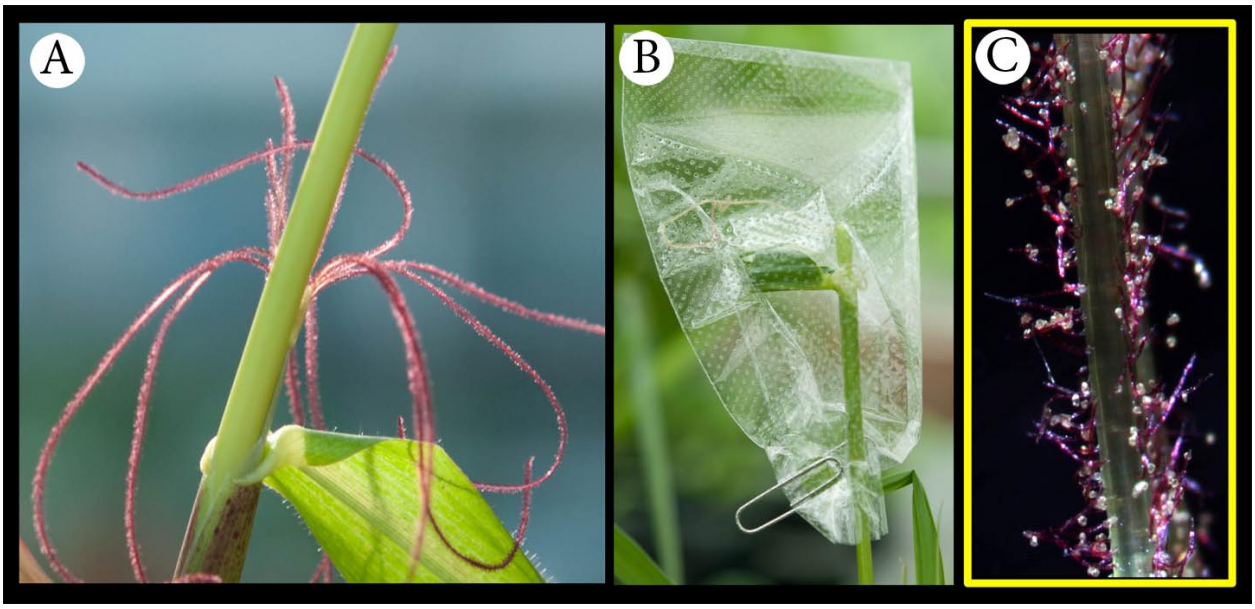

Figure A.1: **Female inflorescence of *Zea mays* subsp. *parviglumis*.** **A**. Elongated stigmas (silks) emerge from the prophylls that enclose the inflorescence. **B**. Stigmas of the female florets were cut back and enclosed with a transparent plastic bag one day before hand pollination. **C**. Pollen were adhered to the stigma papillae after hand pollination.

Appendix B

Three-dimensional reconstruction of mature Balsas teosinte female gametophyte

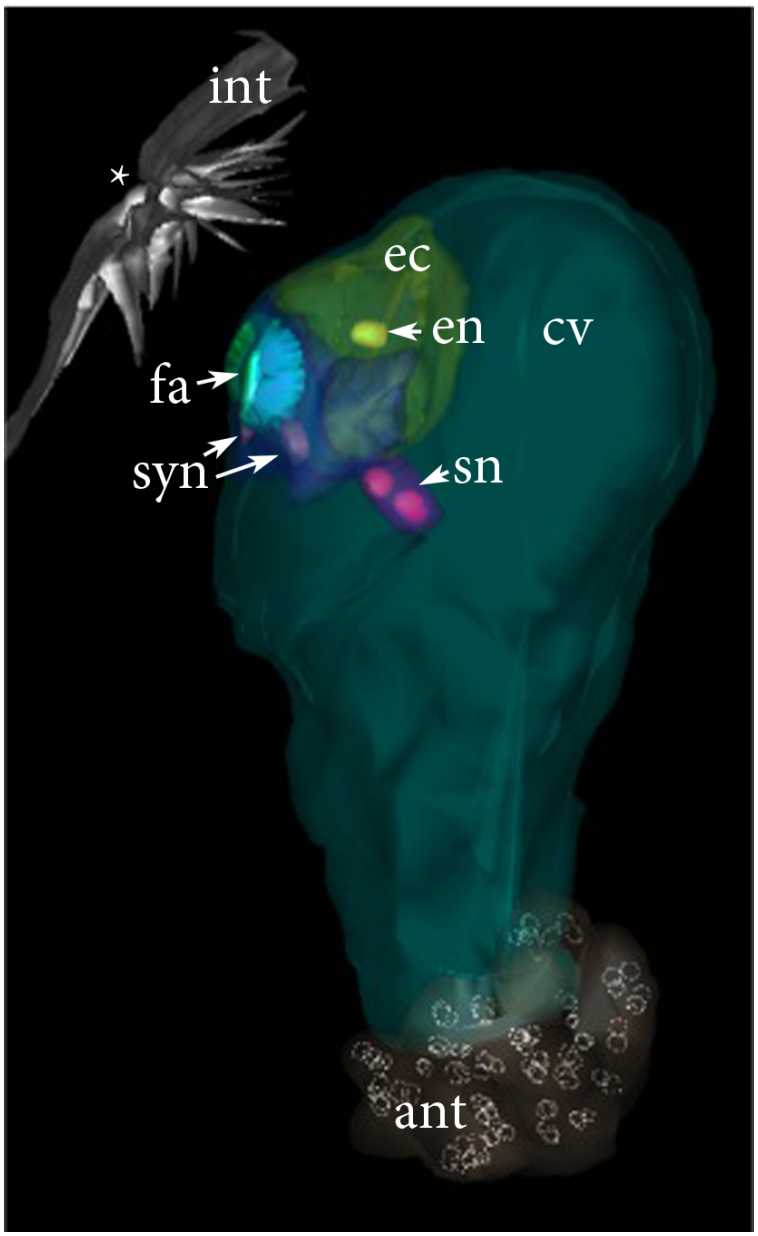

Figure B.1: **Three-dimensional reconstruction of mature female gametophyte of *Zea mays* subsp. *parviglumis*.** The three-dimensional model is oriented so that the micropylar end of the female gametophyte is on the top and the chalazal end on the bottom. The central vacuole (green) occupies the majority of a central cell, and cytoplasm is confined to the peripheral region against the wall of a central cell. Synergid cells (blue) with filiform apparatus (light blue) and an egg cell (yellow), are located right below the micropyle. Antipodal cells (brown) are highly vacuolate. A conspicuous micropyle (black *) formed by inner integuments is right above the micropylar end of the female gametophyte. ant: antipodal cell; cv: central vacuole; filliform apparatus: fa; ec: egg cell; en: egg nucleus; int: inner integument; nu: nucellus; sn: secondary nucleus; syn: synergids nucleus. Dash-line circles in antipodal cells indicate antipodal cell nucleus. Nucellar cells surrounding the female gametophyte are not shown. IMOD software package was used to construct the three dimensional model (Kremer et al., 1996).

Appendix C

Coefficient of relatedness between reproductive components and relatedness ratios of monosporic 3N endosperm in different fertilization types

Table C.1: **Coefficient of relatedness between reproductive components and relatedness ratios of monosporic 3N endosperm in different fertilization types in outcrossing species**

			Origin of paternal genomic contribution through outcrossing				
			Unrelated father			Same father	
Type of fertilization	r*(En→CEm)	r*(MS→En)	r*(MS→Em)	r(En→OEm)	r(En→CEm)/r(En→OEm)	r(En→OEm)	r(En→CEm)/r(En→OEm)
Homofertilization	1	2/3	1/2	1/3	3	1/2	2
Heterofertilization	2/3	2/3	1/2	1/3**	2	1/2**	4/3

(Note: r: coefficient of relatedness, proportion of genome of an individual in common shared by the other individual descending from common parents; En: endosperm; CEm: compatriot embryo; OEm: another embryo in the other seeds on the same maternal plant; MP: maternal plant; r(En→CEm) / r(En→OEm): the ratio of relatedness of an endosperm to its compatriot embryo (CEm) and that to another embryo (OEm) on the same maternal plant; $*$ the same value of r in outcross with unrelated father or with the same father; $**$ coefficient of relatedness of endosperm in heterofertilized seed to other embryos in homofertilized seed)

Table C.2: **Coefficient of relatedness between reproductive components and relatedness ratios of monosporic 3N endosperm in different fertilization types in true-inbreeding species**

			Origin of paternal genomic contribution through outcrossing				
			Unrelated father			Same father	
Type of fertilization	r*(En→CEm)	r*(MS→En)	r*(MS→Em)	r(En→OEm)	r(En→CEm)/r(En→OEm)	r(En→OEm)	r(En→CEm)/r(En→OEm)
Homofertilization	1	1	1	$2/3^{**}$	3/2	1^{**}	1
Heterofertilization	2/3	1	1	$2/3^{***}$	1	1^{***}	2/3

(Note: r: coefficient of relatedness, proportion of genome of an individual in common shared by the other individual descending from common parents; En: endosperm; CEm: compatriot embryo; OEm: another embryo in the other seeds on the same maternal plant; MP: maternal plant; r(En→CEm) / r(En→OEm): the ratio of relatedness of an endosperm to its compatriot embryo (CEm) and that to another embryo (OEm) on the same maternal plant; $*$ the same value of r in outcross with unrelated father or with the same father; $**$ coefficient of relatedness of endosperm in homofertilized seed to other embryos in homofertilized seed; $***$coefficient of relatedness of endosperm in heterofertilized seed to an embryo in a homofertilized seed)

Appendix D

Experimental crosses with the pedigrees

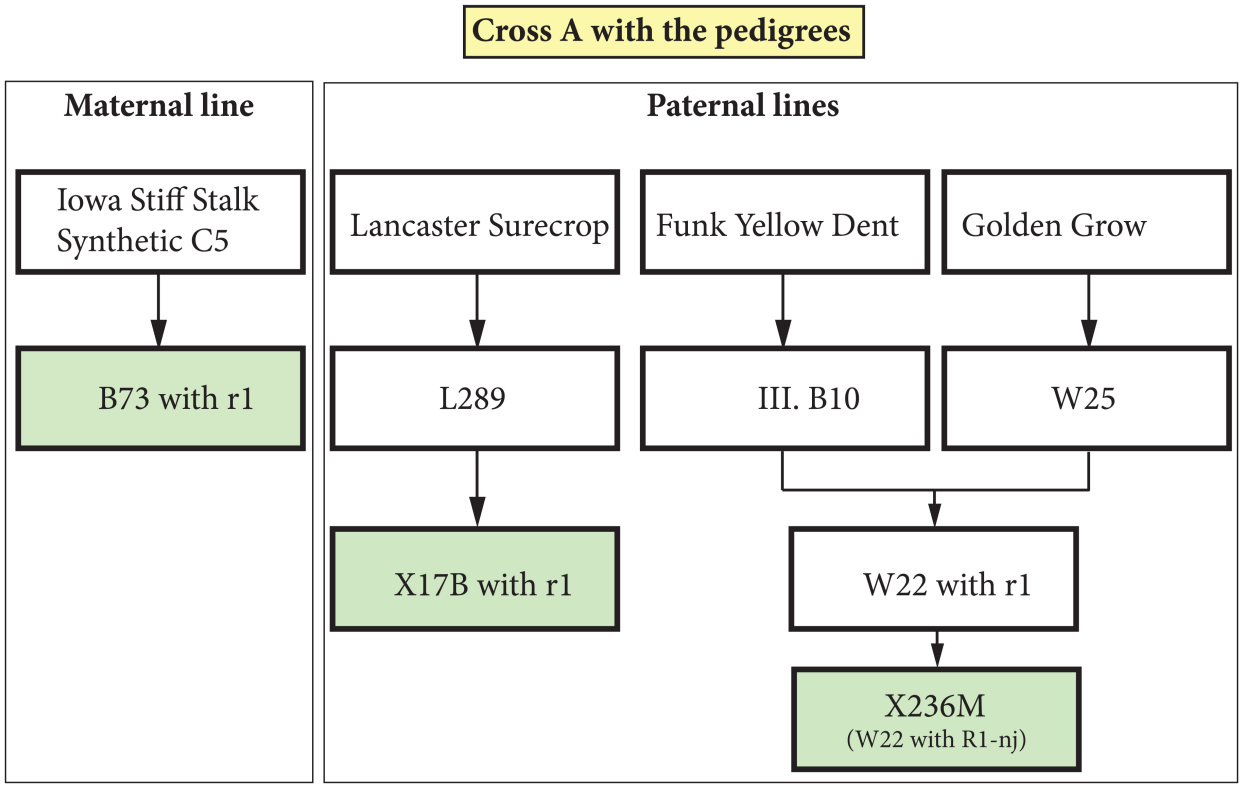

Figure D.1: **Experimental cross A with the pedigree.**

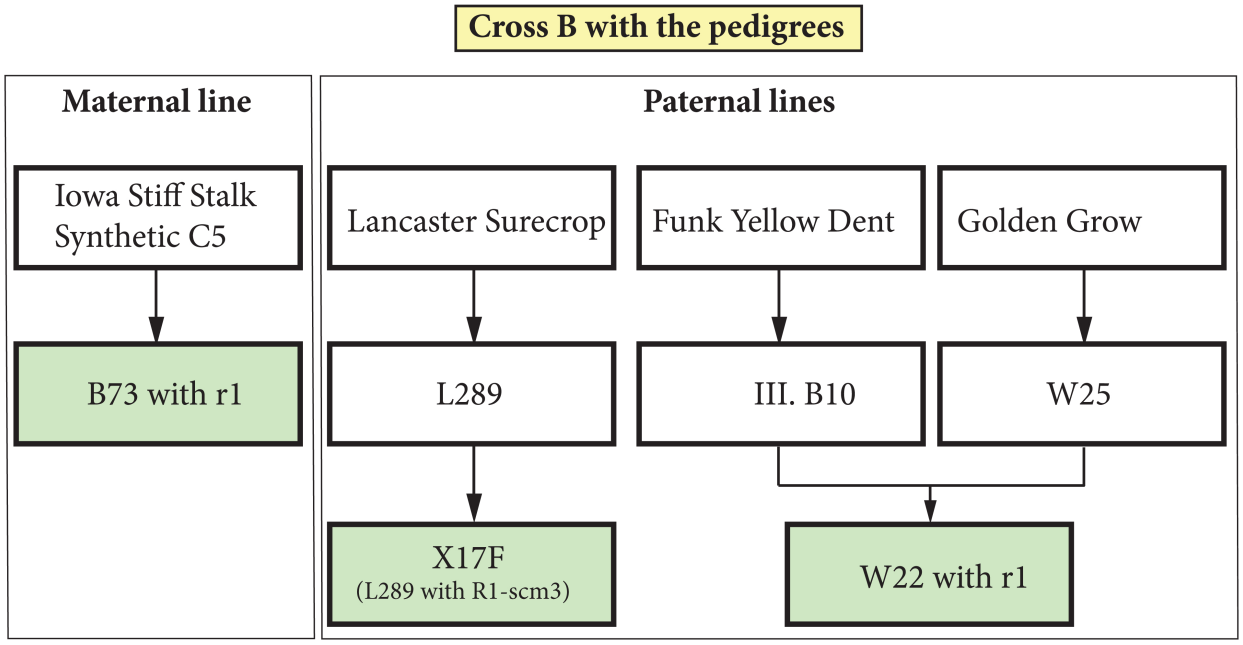

Figure D.2: **Experimental cross B with the pedigree.**

Appendix E

Picture of a maize cob for the reference of kernel locations

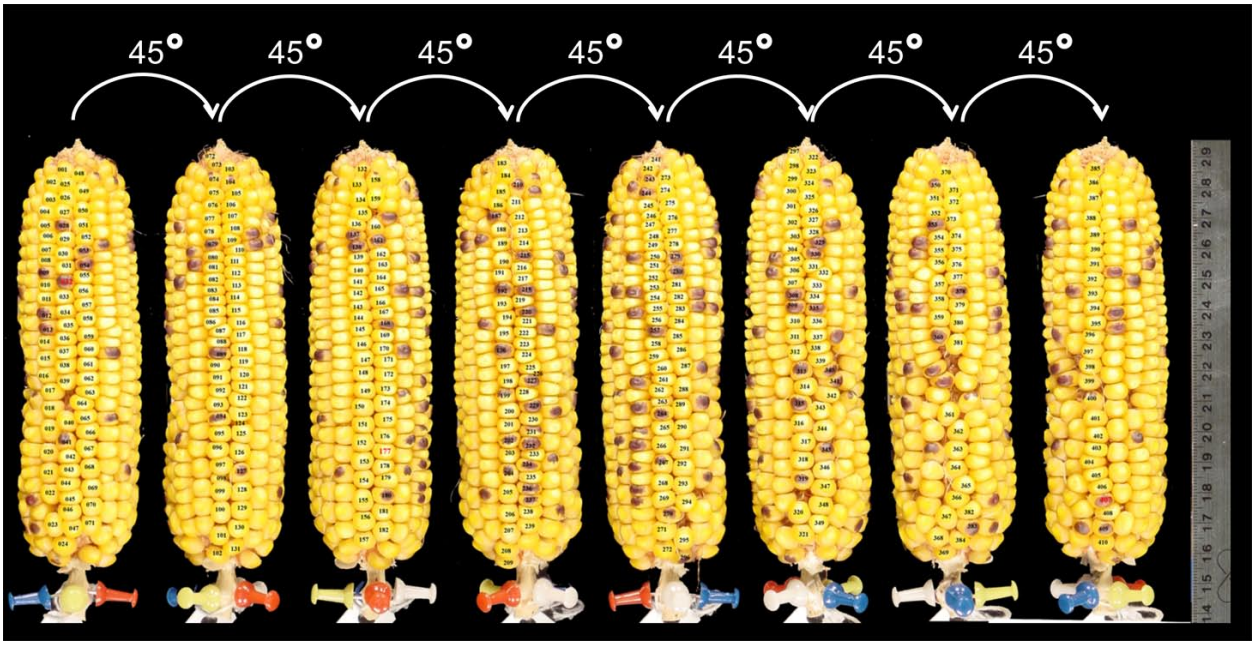

Figure E.1: **Picture of a maize cob for the reference of kernel locations.** To the the location of each kernel on a cob, pictures of a cob were taken every 45 degrees. Serial number was assigned to each kernel, which is corresponding to the number written on the kernel.

Appendix F

Contrast codes of fixed-effect factors in mixed-effect models

Table F.1: **Contrast codes for the state of R1 locus, genetic background of embryos and background of endosperms in mixed effect models**

Contrast code	-1	+1
State of R1 locus (R)	Recessive	Dominant
Embryo genomic background	W22	L289
Endosperm genomic background	W22	L289

Table F.2: **Contrast codes of the fertilization type (FT) in mixed effect models**

Contrast code	-1	+1	0
Fertilization type(FT)	YP	YY	PP